R-02-43

# Reflection seismic studies in the Forsmark area – stage 1

Christopher Juhlin, Björn Bergman and Hans Palm

Uppsala University
Department of Earth Sciences

October 2002

**Svensk Kärnbränslehantering AB**
Swedish Nuclear Fuel
and Waste Management Co
Box 5864
SE-102 40 Stockholm Sweden
Tel 08-459 84 00
+46 8 459 84 00
Fax 08-661 57 19
+46 8 661 57 19

ISSN 1402-3091
SKB Rapport R-02-43

# Reflection seismic studies in the Forsmark area – stage 1

Christopher Juhlin, Björn Bergman and Hans Palm

Uppsala University
Department of Earth Sciences

October 2002

# Summary

Reflection seismic data were acquired in the Spring of 2002 in the Forsmark area, located about 70 km northeast of Uppsala, Sweden. The Forsmark area has been targeted by SKB as a possible storage site for high level radioactive waste. About 16 km of high resolution seismic data were acquired along five separate profiles varying in length from 2 to 5 km. Nominal source and receiver spacing was 10 m with 100 active channels when recording data from a dynamite source (15 -75 g). The profiles were located within a relatively undeformed lens of bedrock that trends in the NW-SE direction. The lens is surrounded by highly deformed rock on all sides. In conjunction with the reflection component of the study, all shots were also recorded on up to eleven 3-component fixed Orion seismographs. These recordings provided long offset data from which a velocity model of the uppermost 400 m of bedrock could be derived.

Results from the study show that the bedrock has been well imaged down to depths of at least 3 km. The upper 1000 m of bedrock is much more reflective in the south-eastern portion of the lens compared to the northwestern part close to the Forsmark reactors. This is interpreted as the bedrock being more homogeneous in the northwest. However, a major reflective zone (the A1 reflector) is interpreted to dip to the S-SE below this homogeneous bedrock. In the southeastern portion of the lens the orientation of the reflectors is well determined where the profiles cross one another. The general strike of the major reflectors is NE-SW with dips of 20-35 degrees to the southeast.

# Contents

# 1. Introduction

Seismic data were acquired in the Forsmark area in northeastern Uppland (Figure 1-1) during the months of March, April and May in the year 2002 by Uppsala University under contract from SKB. Approximately 16 km of high-resolution (10 m shot and receiver spacing) reflection seismic data were acquired along 5 different profiles (Figures 1-2 and 1-3) using about 1300 shot points. Most of these shots were also recorded on a stationary network of 11 Orion 3-component seismometers (Figure 1-3). The reflection seismic method used here imaged the bedrock from the near surface (upper tens of meters) down to depths of several km. Zones or changes in the elastic properties of the bedrock, i.e. lithological changes or fracture zones, greater than about a meter in thickness and dipping up to 60-70º were imaged. First arrival picks from the Orion stations allowed an average 1D velocity function down to 400 m to be determined. The picks were also used to estimate the large scale 3D seismic velocity structure in the upper 500 m.

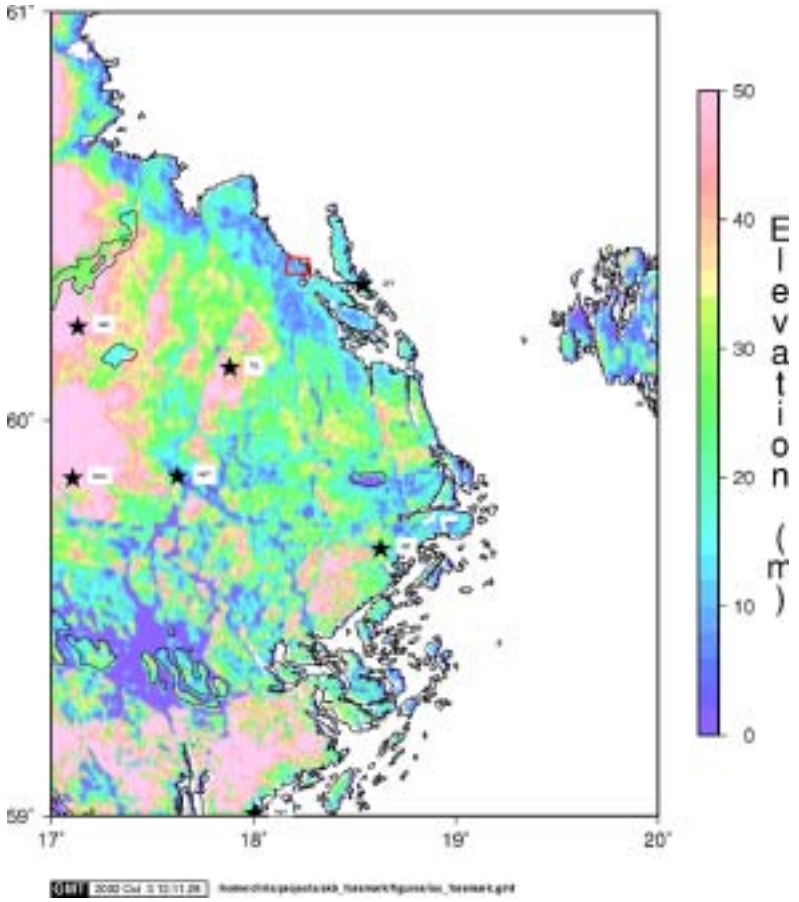


*Figure 1-1. Location of study area (red box). Permanent seismological stations of the Swedish Seismological Network are marked by stars.*


*Figure 1-2. General location of the seismic reflection profiles relative to the Forsmark nuclear power plant.*

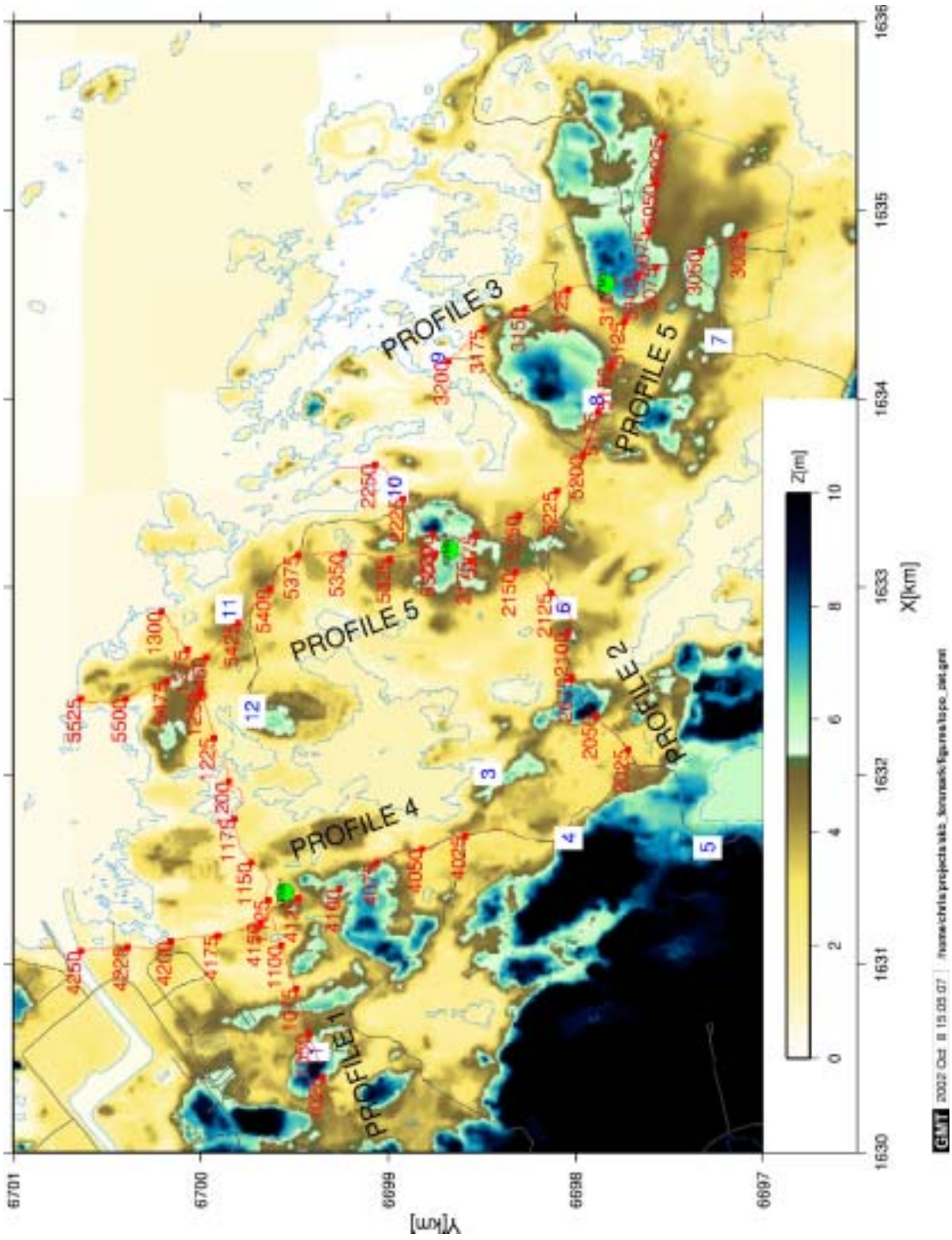


*Figure 1-3. Exact location of seismic reflection profiles (red lines) and Orion seismic stations (blue numbers). Location of the first three planned deep borehole shown as green circles.*

# 2. Data acquisition

The acquisition crew arrived in the field on 7 March and data acquisition began on 10 March, 2002 using the acquisition parameters given in Table 2-1. Data acquisition finished on 5 May, 2002 followed by 5 days of demobilization and cleanup. During the acquisition period there were 14 days that no data were acquired due to moving of profiles or bad weather.

Shot points and geophones were located as much as possible on bedrock. Shotholes were drilled at the closest suitable location to a staked point where bedrock was present, but not further from the staked point than 30 cm parallel and 1 m perpendicular to the profile. If no bedrock was found within this area, even after removing 50 cm of soil, the shothole was drilled at the staked point. In bedrock, 12 mm diameter shotholes were drilled to 90 cm depth with an electric drilling machine powered by a gasoline generator. Charges of 15 g were used in bedrock shotholes. In soil cover, 32 mm diameter shotholes were drilled to 150 cm depth with an air pressure drill. These holes were cased with a plastic or metal casing with an inner diameter of 16.9 mm (plastic) or 18 mm (metal). Charges of 75 g were used in these holes. Bedrock shotholes were used on only about 5 % of the profiles. Geophones were placed in drilled bedrock holes wherever possible, otherwise they were placed directly in the soil cover. All shotholes and geophone locations were surveyed with high precision GPS instruments in combination with a total station. This combination gave a horizontal and vertical precision of better than 10 cm.

For tomographic data, a maximum of 11 Orion station were in operation at the same time, see Table 2-1. The stations were positioned on bedrock outcrop in such a pattern to produce the best coverage while still being accessible by road. Every station consisted of one Orion portable seismograph and data recorder, one 3-component seismometer, one GPS-antenna and one car- battery powering the Orion.

The Orion portable seismograph records data onto a hot swappable hard drive. These hard drives were retrieved each day after shooting was finished. Data were recorded continuously on the hard drives, however, only 20 seconds of data from following each shot was extracted from the hard drives and converted to standard SEGY format for archiving. The acquired data was stored on optical back-up every fourth day and transported to Uppsala University.

Data quality was checked and documented in the observers log. From the quality check it was observed that some stations were either not recording data at all, or recording poor quality data. During the first weeks, three stations were moved a few meters in order to increase data quality. For several stations there were problems with either GPS-antenna, internal battery power, external battery connectors as well as signal cables and signal cables connectors on the Orion. After both repairs in the field and at Uppsala University, 10 Orion stations were operating satisfactorily at the end of the study.

**Table 2-1. Acquisition parameters for the reflection and tomographic seismic components.**

| *Parameter* | *Reflection* | *Orion stations* |
|---|---|---|
| **Spread type** | End-on, shoot through | 11 stations |
| **Number of channels** | 100 | 3 (N-S, W-E, Z) |
| **Near offset** | 20 m | NA |
| **Geophone spacing** | 10 m | NA |
| **Geophone type** | 28 Hz single | 0.2 Hz / 1 Hz |
| **Shot spacing** | 10 m | 10 m |
| **Charge size** | 15/75 gram | 15/75 gram |
| **Nominal charge depth** | 0.9/1.5 m | 0.9/1.5 m |
| **Nominal fold** | 50 | 1 |
| **Recording instrument** | SERCEL 348 | Orion |
| **Sample rate** | 1 ms | 2 ms |
| **Field low cut** | 8 Hz | Out |
| **Field high cut** | 250 Hz | 125 Hz |
| **Record length** | 4 seconds | 20 s |
| **Profile length / shots** | 1- 2950 m / 260 | 1- 2950 m / 260 |
| | 2- 2740 m / 217 | 2- 2740 m / 217 |
| | 3- 2050 m / 143 | 3- 2050 m / 143 |
| | 4- 2410 m / 196 | 4- 2410 m / 196 |
| | 5- 5280 m / 507 | 5- 5280 m / 507 |

# 3. Data processing

## 3.1. Reflection seismic processing

### *3.1.1. CDP Lines*

The reflection seismic data were acquired along crooked lines. CDP stacking lines were chosen that were piece-wise straight. The data were projected on to the lines prior to stacking (Figure 3-1). The stacks shown in this report refer to the CDP number along these lines. Station numbers are also shown on the stacks, but these are only approximate. A plot of just the CDP lines on the topography is shown in Figure 3-2.

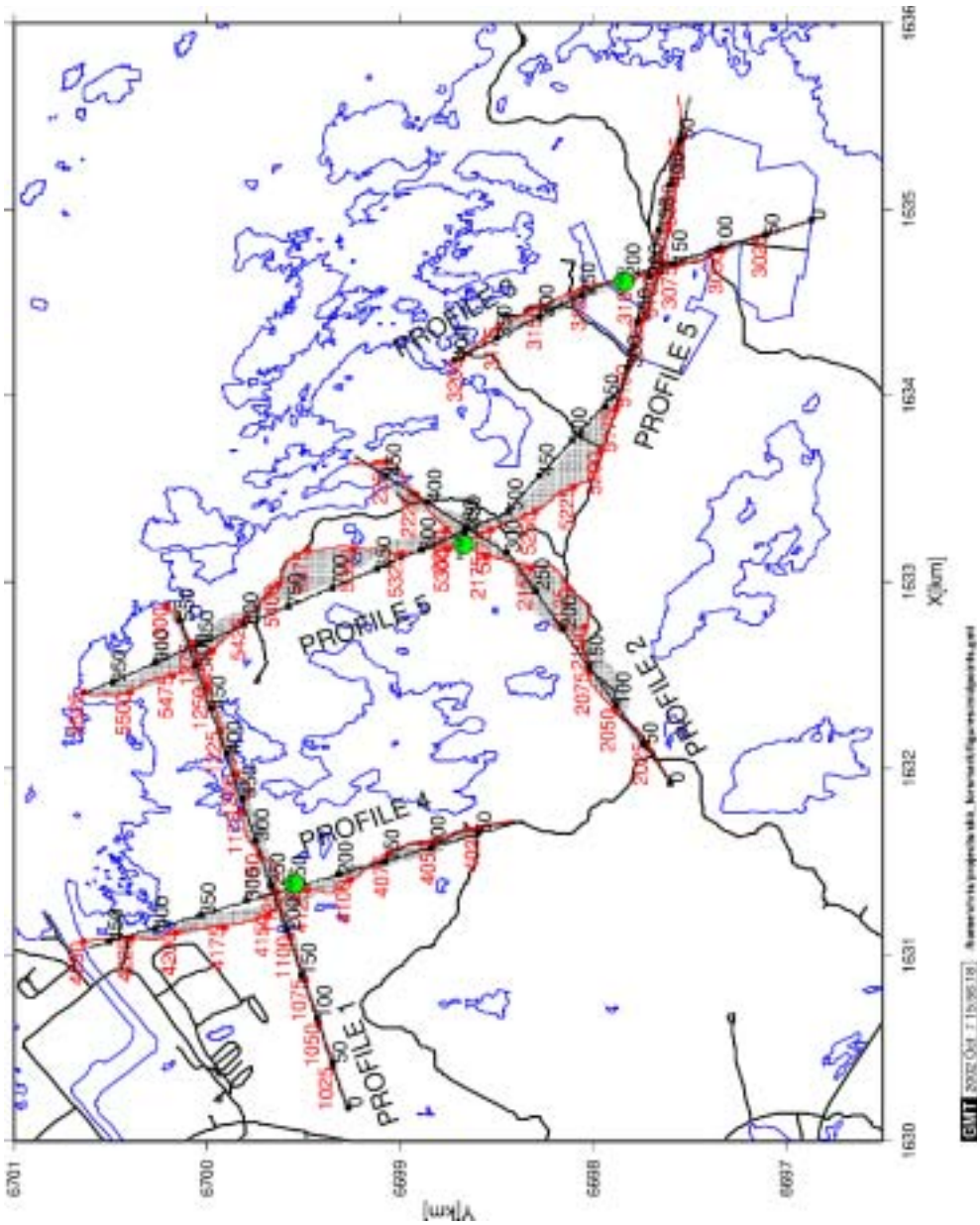


*Figure 3-1. Midpoints between shots and receivers (gray areas) and the CDP lines that the data have been projected onto and stacked along (black). Actual location of the seismic profiles (red) are also shown. Location of the first three planned deep borehole shown as green circles.*

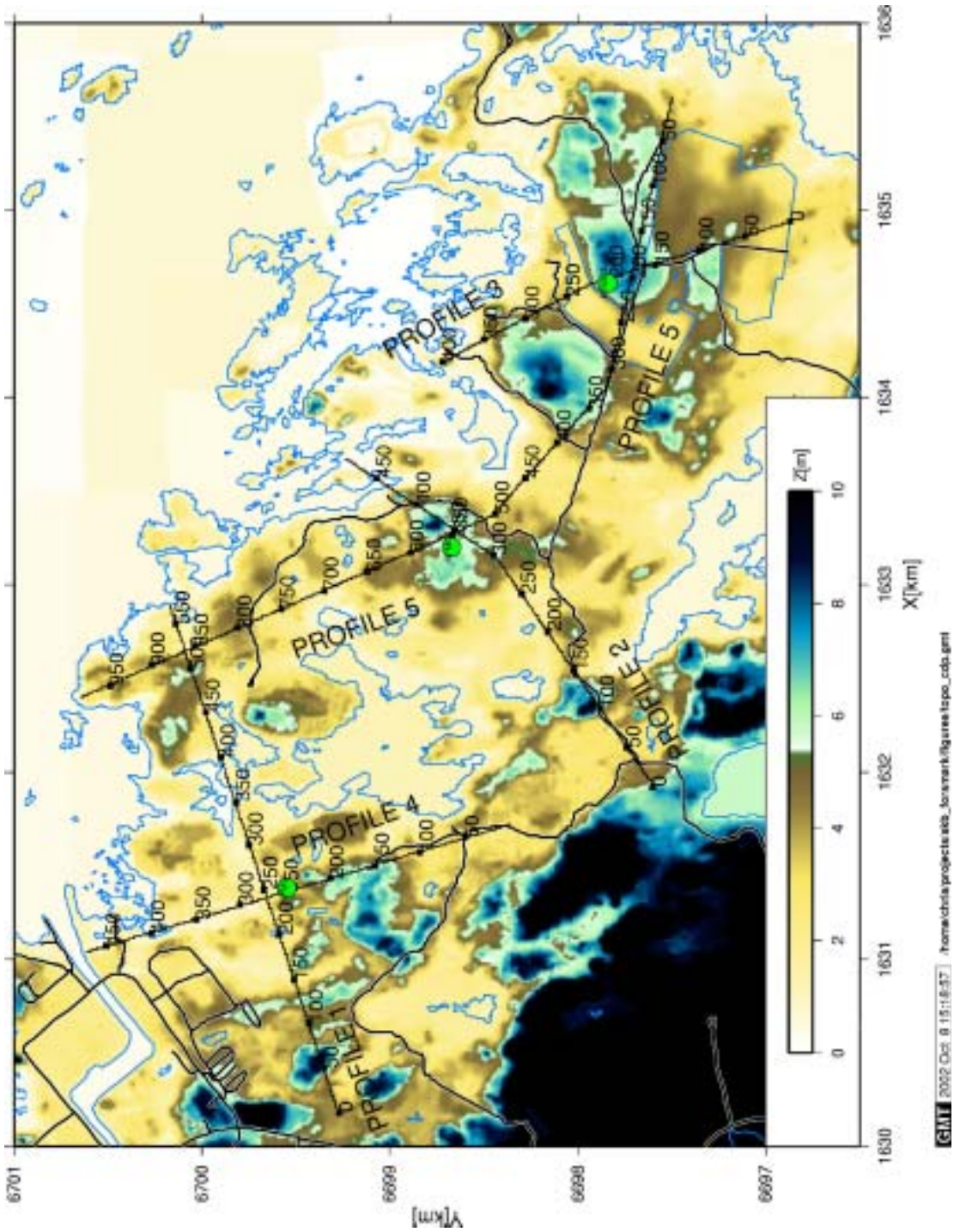


*Figure 3-2. CDP lines plotted on topography. It is these CDP lines the seismic data have been projected onto. Location of the first three planned deep borehole shown as green circles.*

### 3.1.2. Processing parameters

The reflection seismic data were processed with the parameters given in Table 3-1.

**Table 3-1. Processing parameters for the seismic profiles.**

| *Step* | *Process* | |
|---|---|---|
| 1 | Read SEG2 data - 2000 ms | |
| 2 | Spike and noise edit | |
| 3 | Pick first breaks | |
| 4 | Scale by time | |
| 5 | Spectral Whitening | |
| | 50-60-240-270 Hz | |
| | Panels: 12 | |
| | Window: 250 ms | |
| 6 | Bandpass filter | |
| | 70-140-300-450 Hz | 0-200 ms |
| | 60-120-300-450 Hz | 100-400 ms |
| | 50-100-300-450 Hz | 300-2000 ms |
| | Notch: 50, 100 Hz | |
| 7 | Refraction statics | |
| 8 | Trace top mute | |
| | 0 m: 10 ms; 1100 m: 210 ms | |
| 9 | Sort to CDP domain | |
| 10 | Velocity analyses | |
| 11 | Residual statics | |
| 12 | Sort to common offset domain | |
| 13 | AGC - 50 ms window | |
| 14 | NMO | |
| 15 | Common offset F-K DMO | |
| | velocity 0 ms - 5300 m/s, 500-5900, 1000-6000 | |
| 16 | AGC - 50 ms window | |
| 17 | Stack (mean) | |
| 18 | Trace equalization 0-800 ms | |
| 19 | F-X Decon | |

### 3.1.3. Stacked sections

In the figures that follow (Figures 3-3 to 3-13) a stack down to 2 seconds is first shown followed by a more detailed image of the uppermost 0.6 s for each profile. In these figures the data have been processed to step 18 in Table 3-1. The approximate depth scale shown in the figures is based on an average velocity of 5850 m/s and is only valid for true sub-horizontal reflections, not dipping or out-of-the-plane ones.

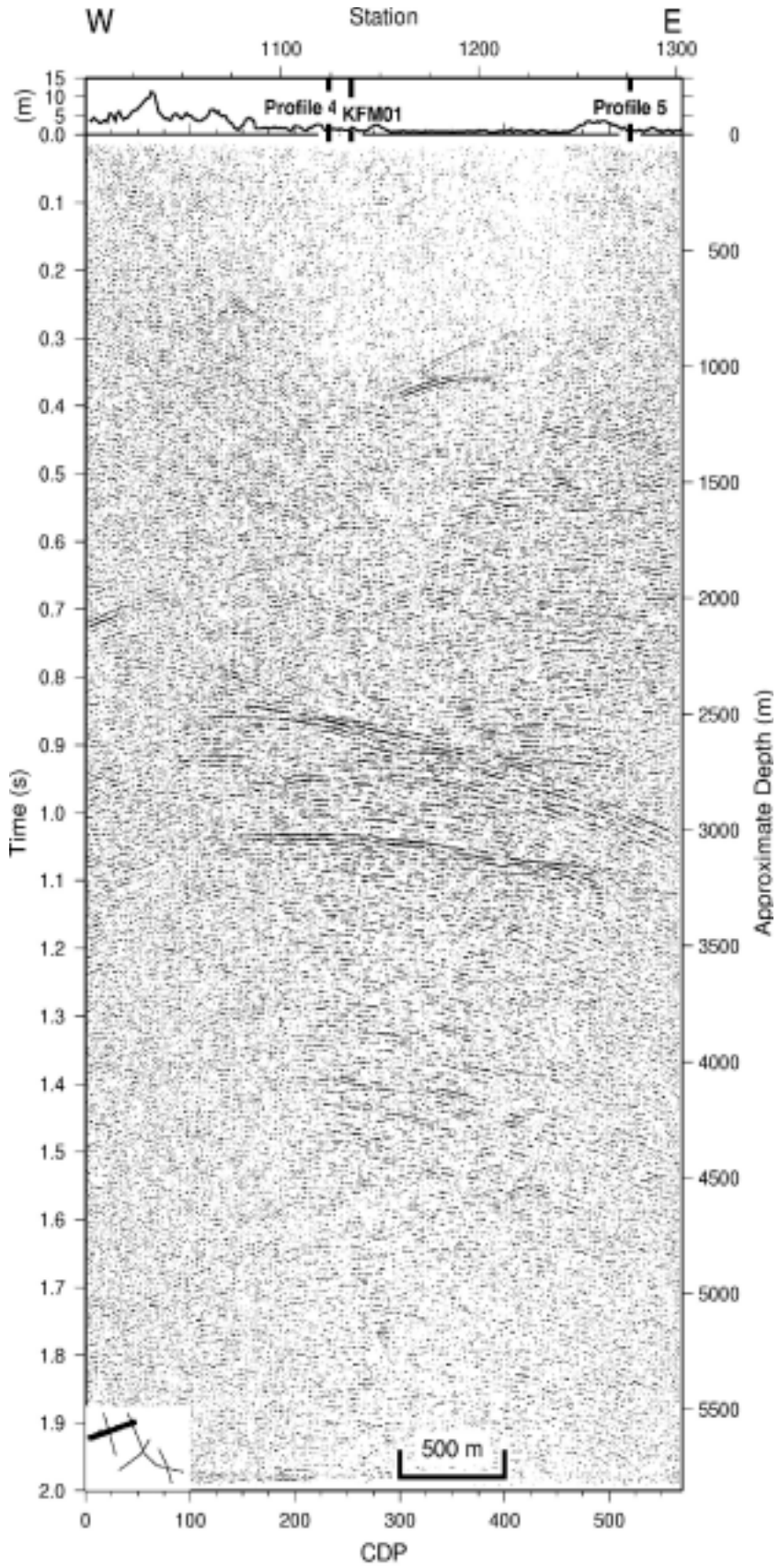


*Figure 3-3. Stacked section of profile 1 down to 2 seconds. Location of section indicated in lower left corner. Depth scale only valid for true sub-horizontal reflections.*

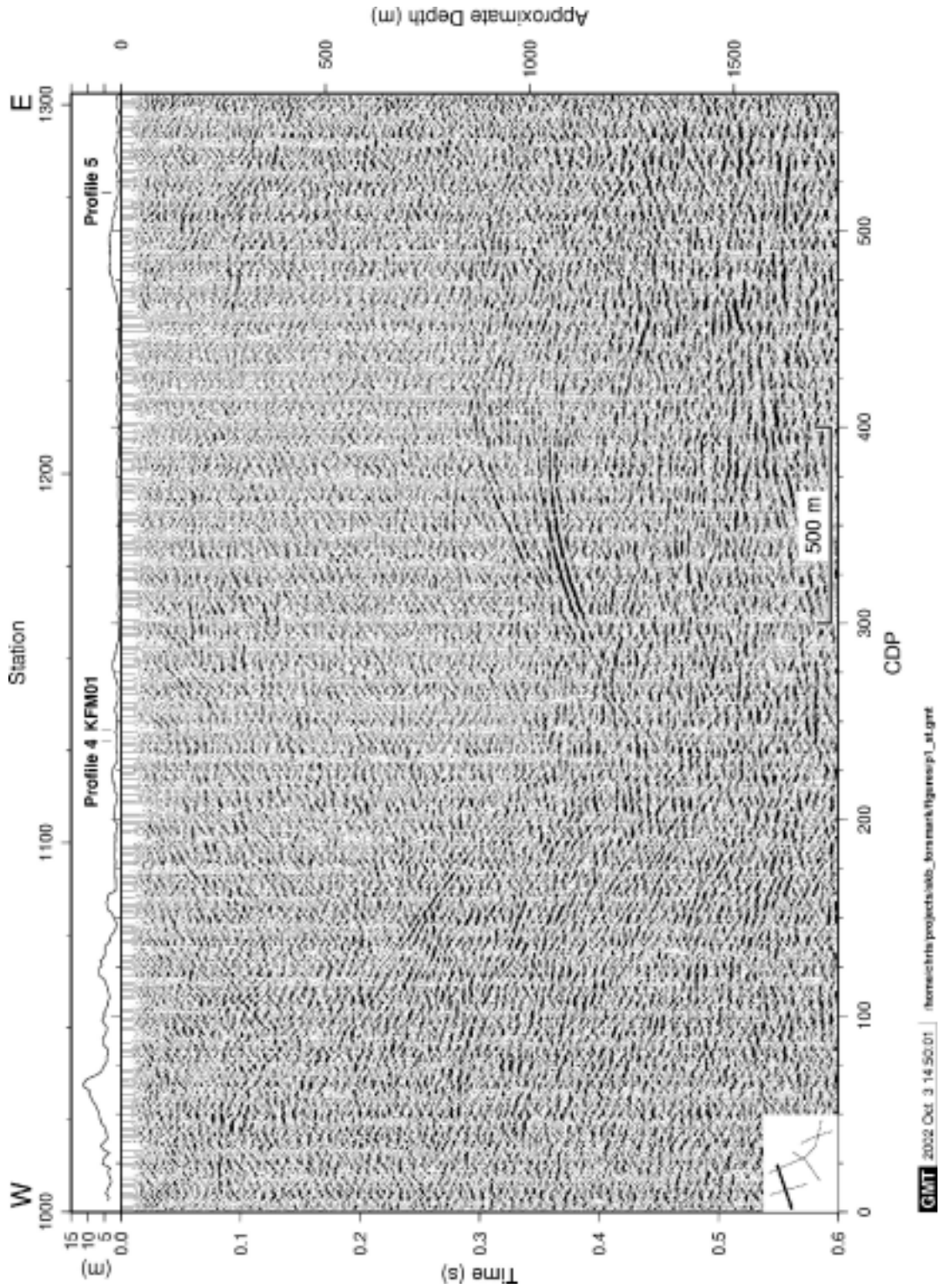


*Figure 3-4. Stacked section of profile 1 down to 0.6 seconds. Location of section indicated in lower left corner. Depth scale only valid for true sub-horizontal reflections*

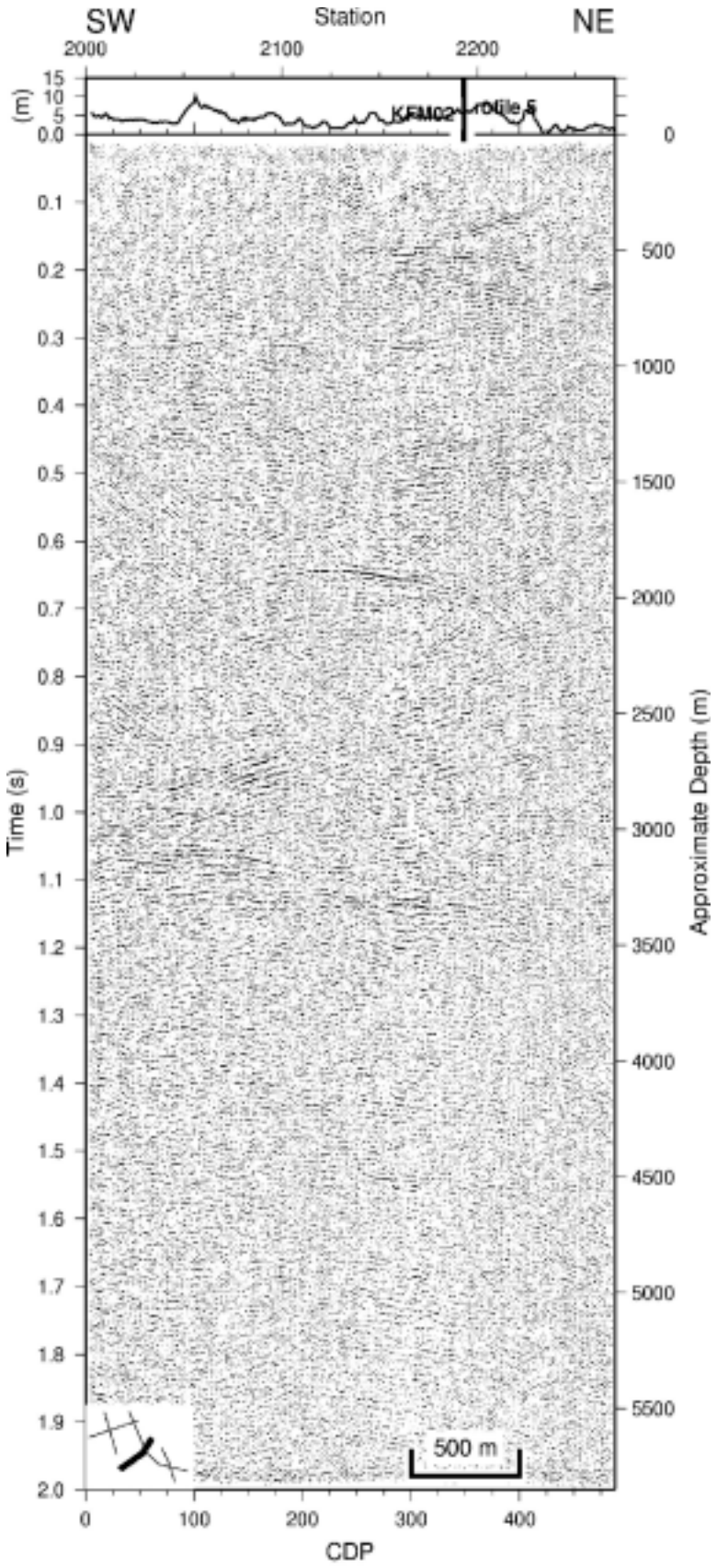


*Figure 3-5. Stacked section of profile 2 down to 2 seconds. Location of section indicated in lower left corner. Depth scale only valid for true sub-horizontal reflections.*

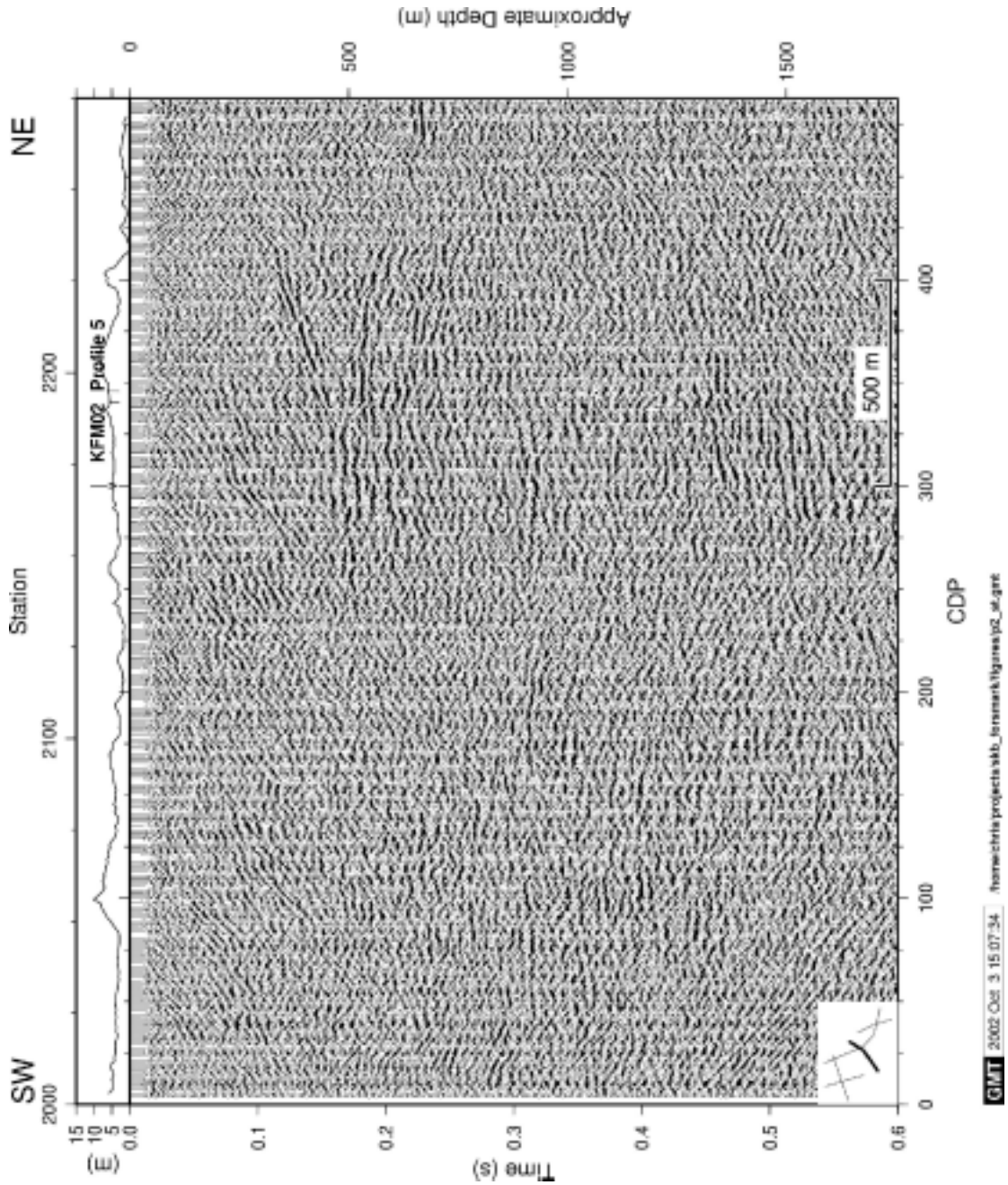


*Figure 3-6. Stacked section of profile 2 down to 0.6 seconds. Downward arrow (↓) indicates where the CDP line bends. Location of section indicated in lower left corner. Depth scale only valid for true sub-horizontal reflections.*

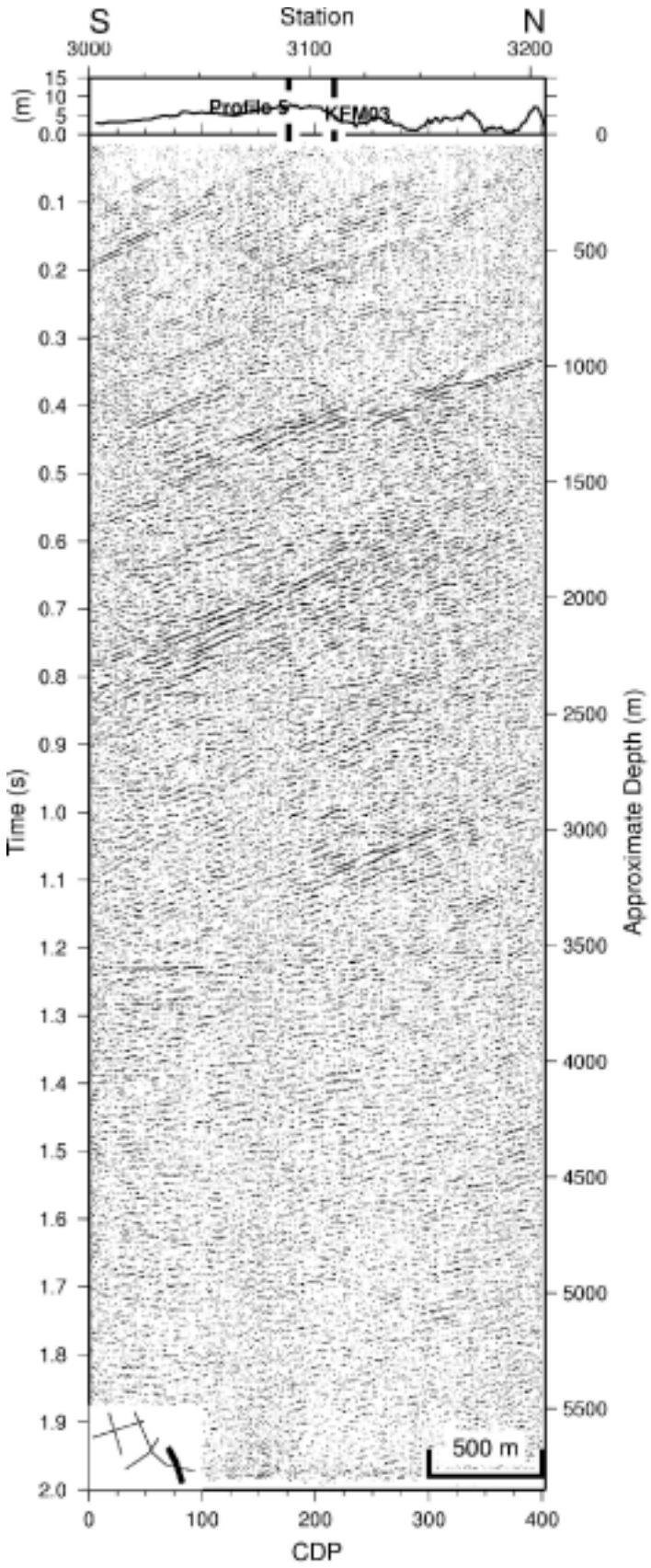


*Figure 3-7. Stacked section of profile 3 down to 2 seconds. Location of section indicated in lower left corner. Depth scale only valid for true sub-horizontal reflections.*

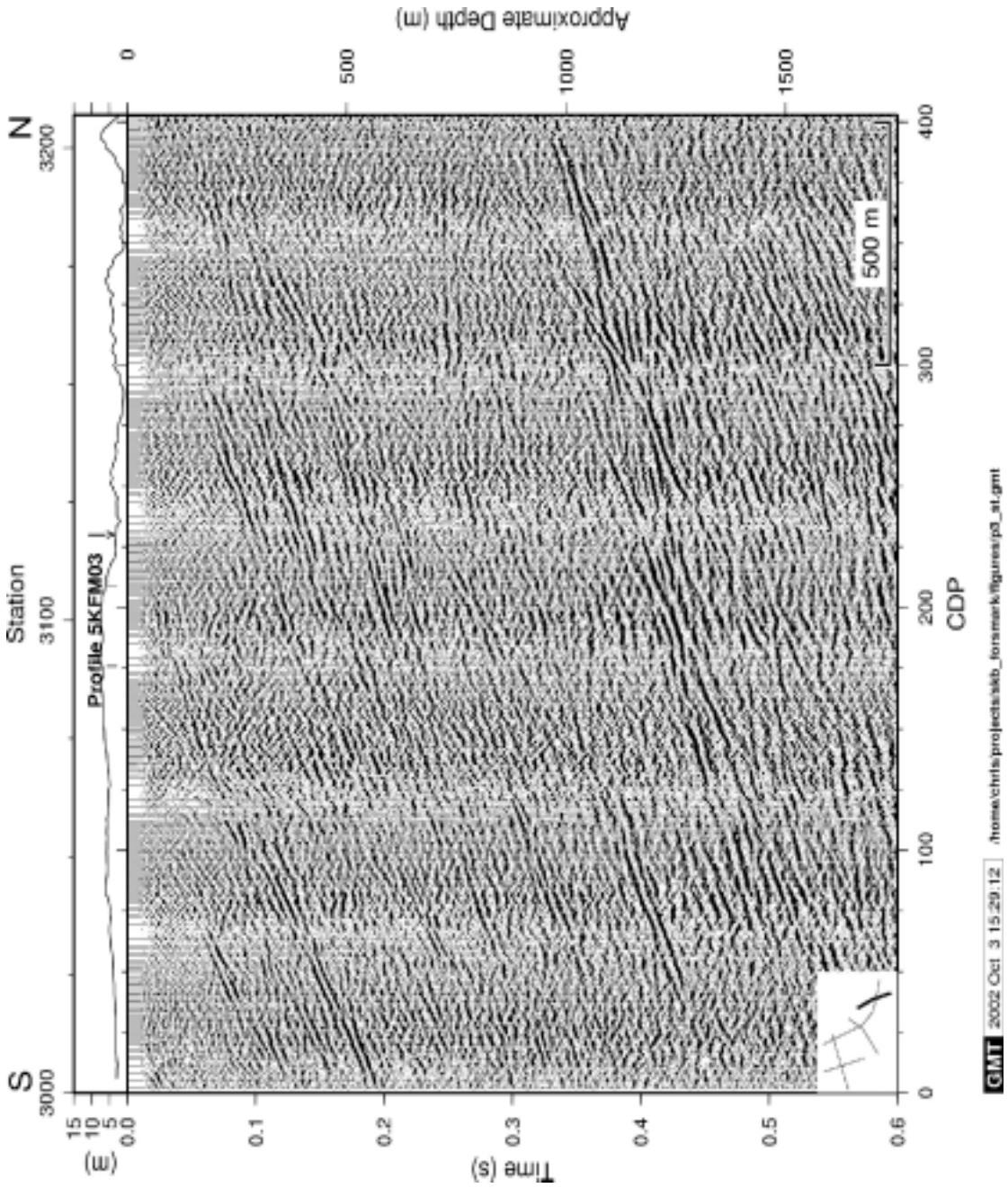


*Figure 3-8. Stacked section of profile 3 down to 0.6 seconds. Downward arrow (↓) indicates where the CDP line bends. Location of section indicated in lower left corner. Depth scale only valid for true sub-horizontal reflections.*

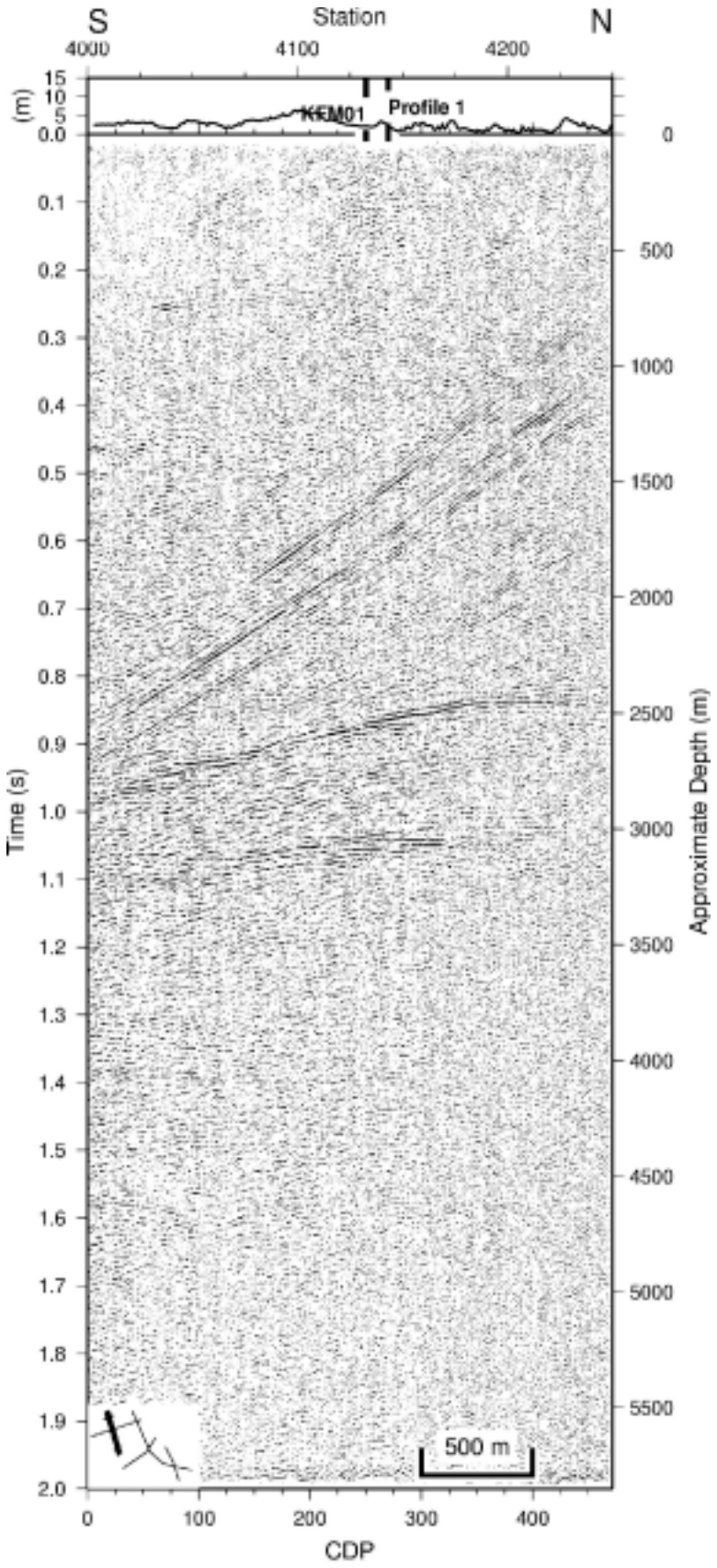


*Figure 3-9. Stacked section of profile 4 down to 2 seconds. Location of section indicated in lower left corner. Depth scale only valid for true sub-horizontal reflections.*

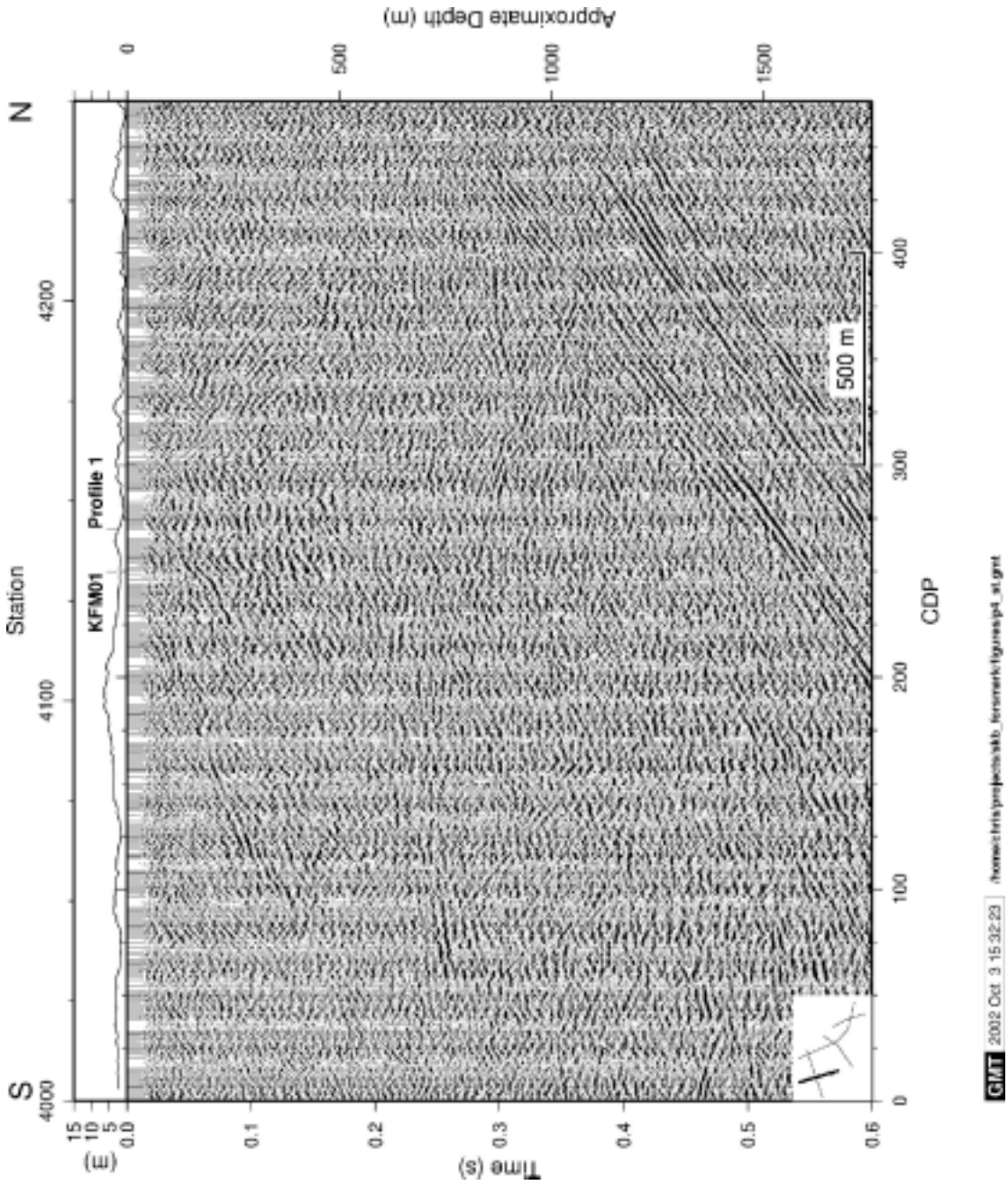


*Figure 3-10. Stacked section of profile 4 down to 0.6 seconds. Location of section indicated in lower left corner. Depth scale only valid for true sub-horizontal reflections.*

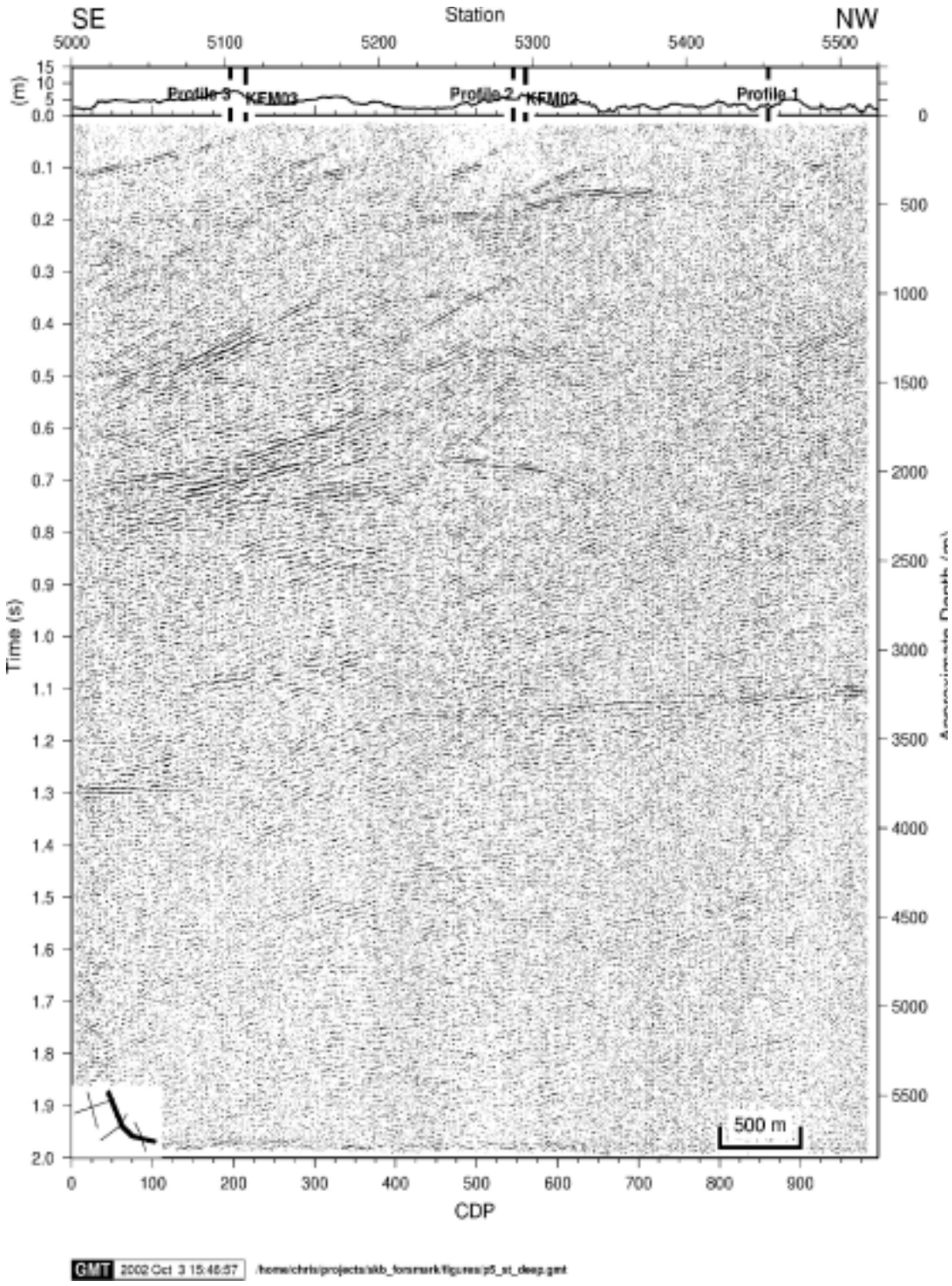


*Figure 3-11. Stacked section of profile 5 down to 2 seconds. Location of section indicated in lower left corner. Depth scale only valid for true sub-horizontal reflections.*

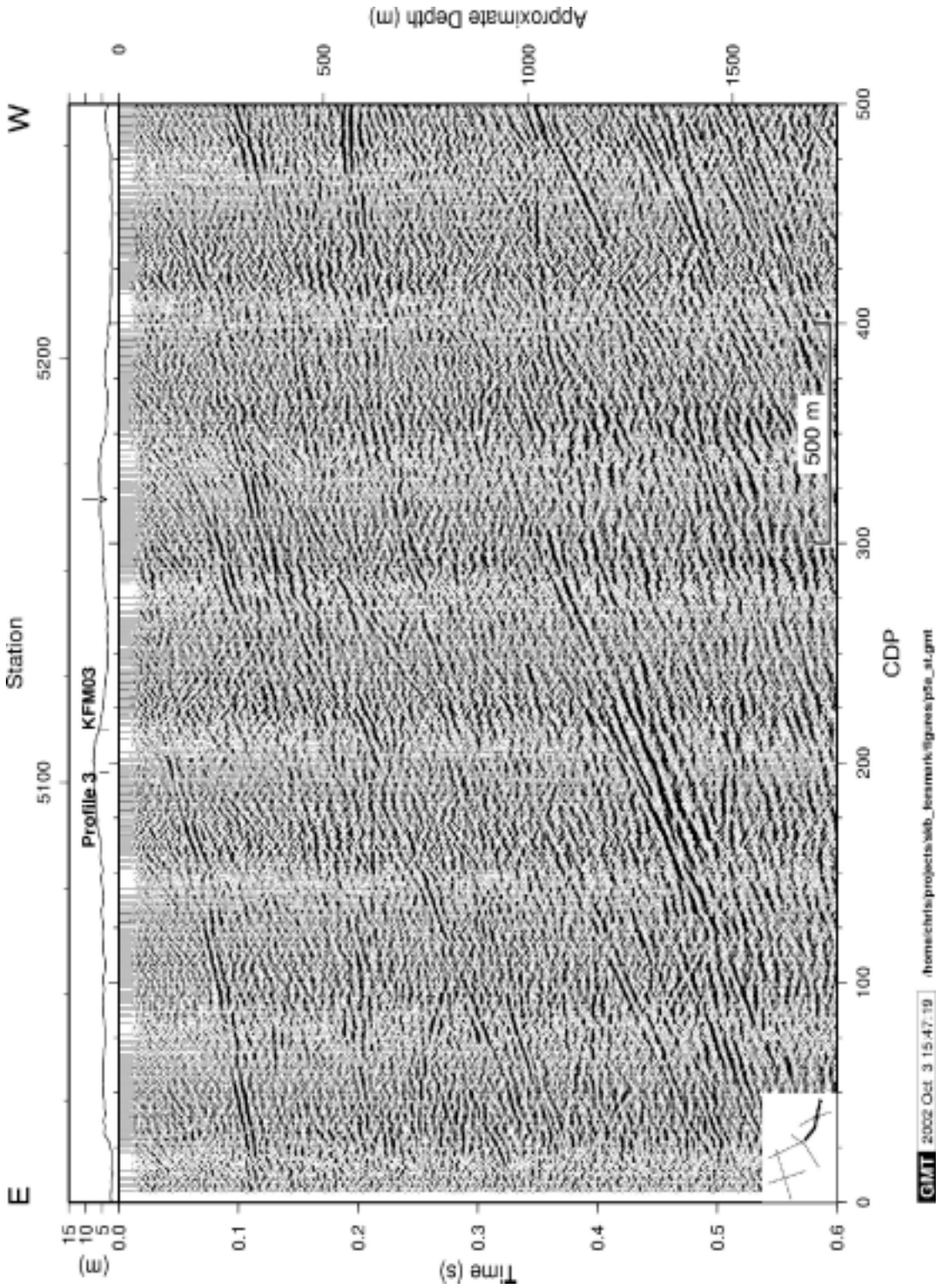


*Figure 3-12. Stacked section of the eastern half of profile 5 down to 0.6 seconds. Downward arrow (↓) indicates where the CDP line bends. Location of section indicated in lower left corner. Depth scale only valid for true sub-horizontal reflections.*

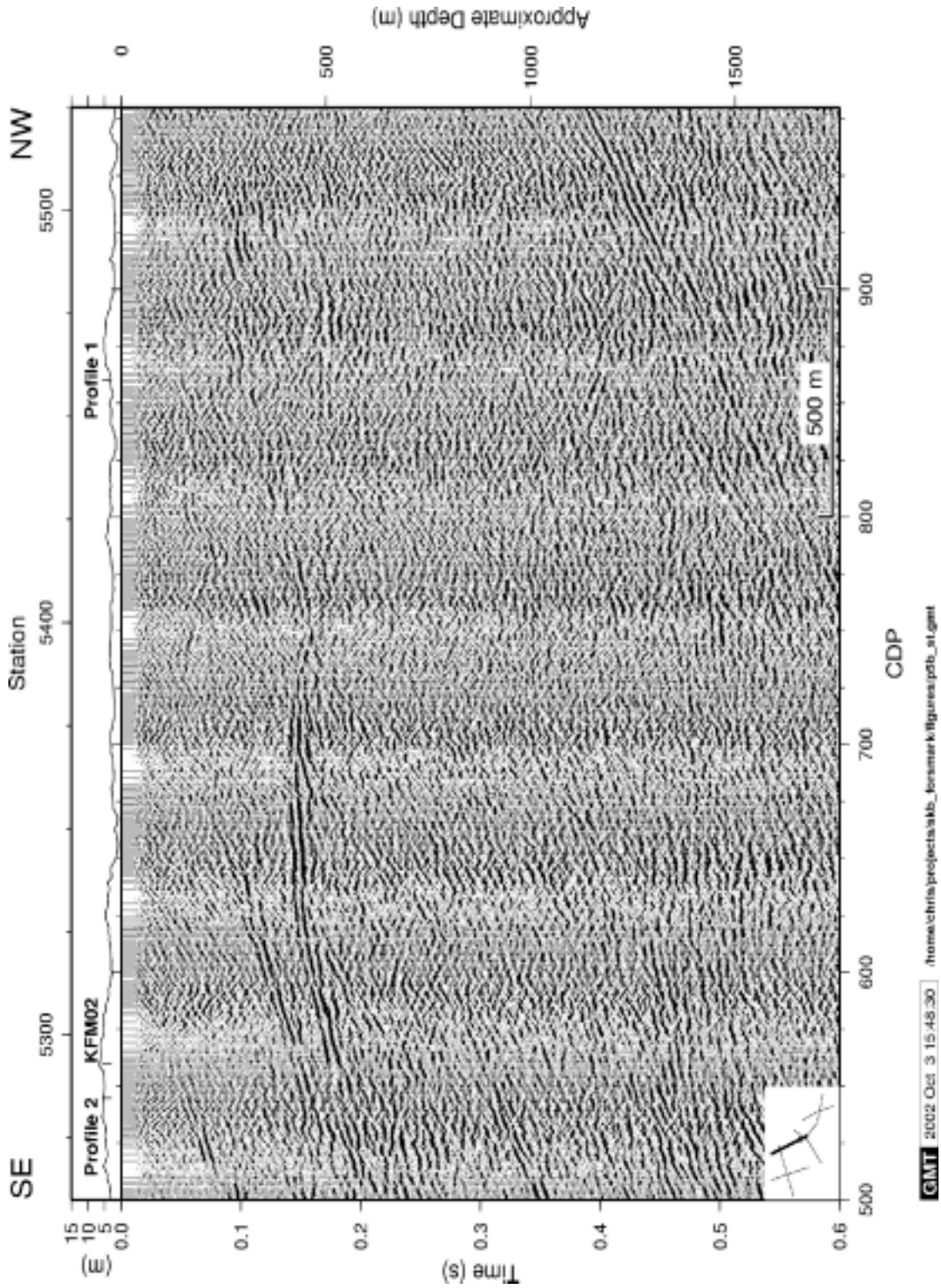


*Figure 3-13. Stacked section of the western half of profile 5 down to 0.6 seconds. Location of section indicated in lower left corner. Depth scale only valid for true sub-horizontal reflections.*

## 3.2. Orion stations

First breaks from the Orion stations are used for estimating the average velocity as a function of depth and for studying 3D variations in the velocity in the area.

Data quality were highly variable on the Orion stations. Some stations showed generally good quality data whereas others did not record usable data for most of the study. The reason for the lack of good quality data on some stations is not entirely clear at present. Station location is important, but technical problems, such as choice of seismometers and cable connections, may also play a role. Figure 3-14 shows a typical example of good quality data from profile 5. First breaks can be picked on most of the shots and clear reflections are observed from shot point 5000 to about shot point 5300.

First breaks have been picked on the Orion stations where the data quality were of sufficient quality. These first breaks plot nearly as a straight line as a function of offset (bottom part of Figure 3-15). When the first breaks are reduced, a value of distance divided by velocity is subtracted, it becomes clear that a velocity gradient exists in the upper few hundred meters of bedrock (top part of Figure 3-15). At offsets of 2000 m the apparent velocity is about 6000 m/s. Results from the inversion of the first break traveltimes are presented in section 4.2.

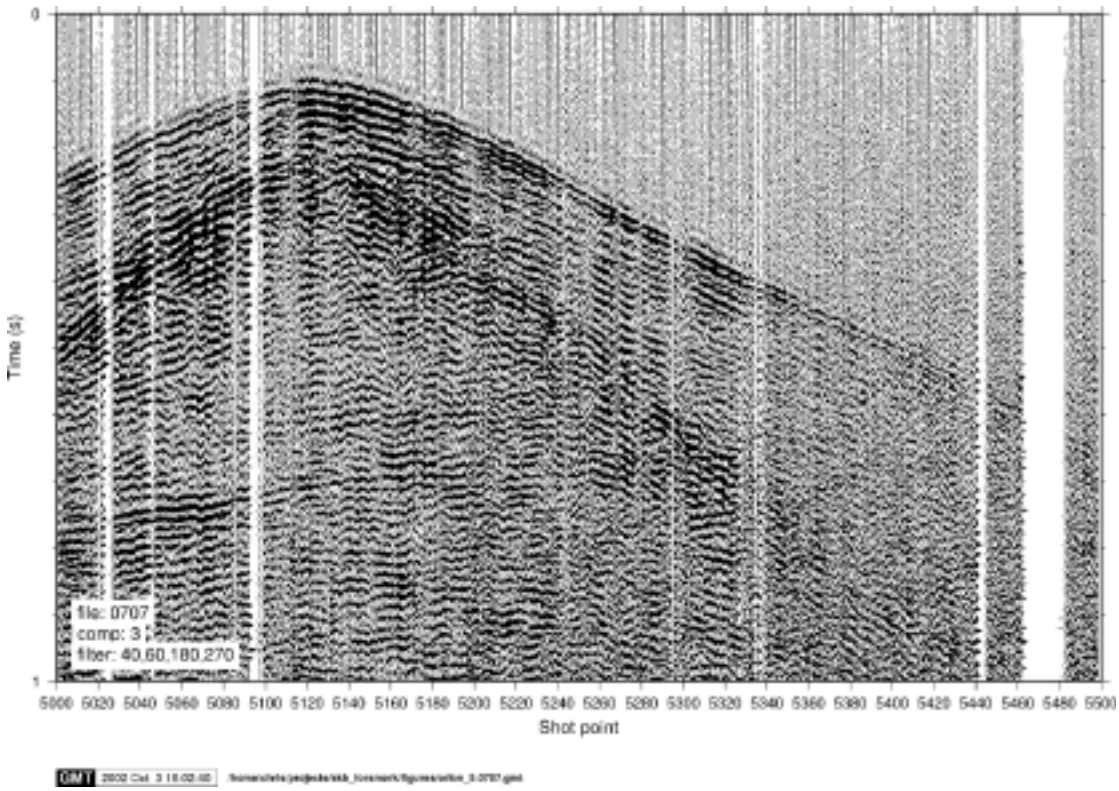


*Figure 3-14. Profile 5 vertical component seismograms recorded at Orion station 7.*

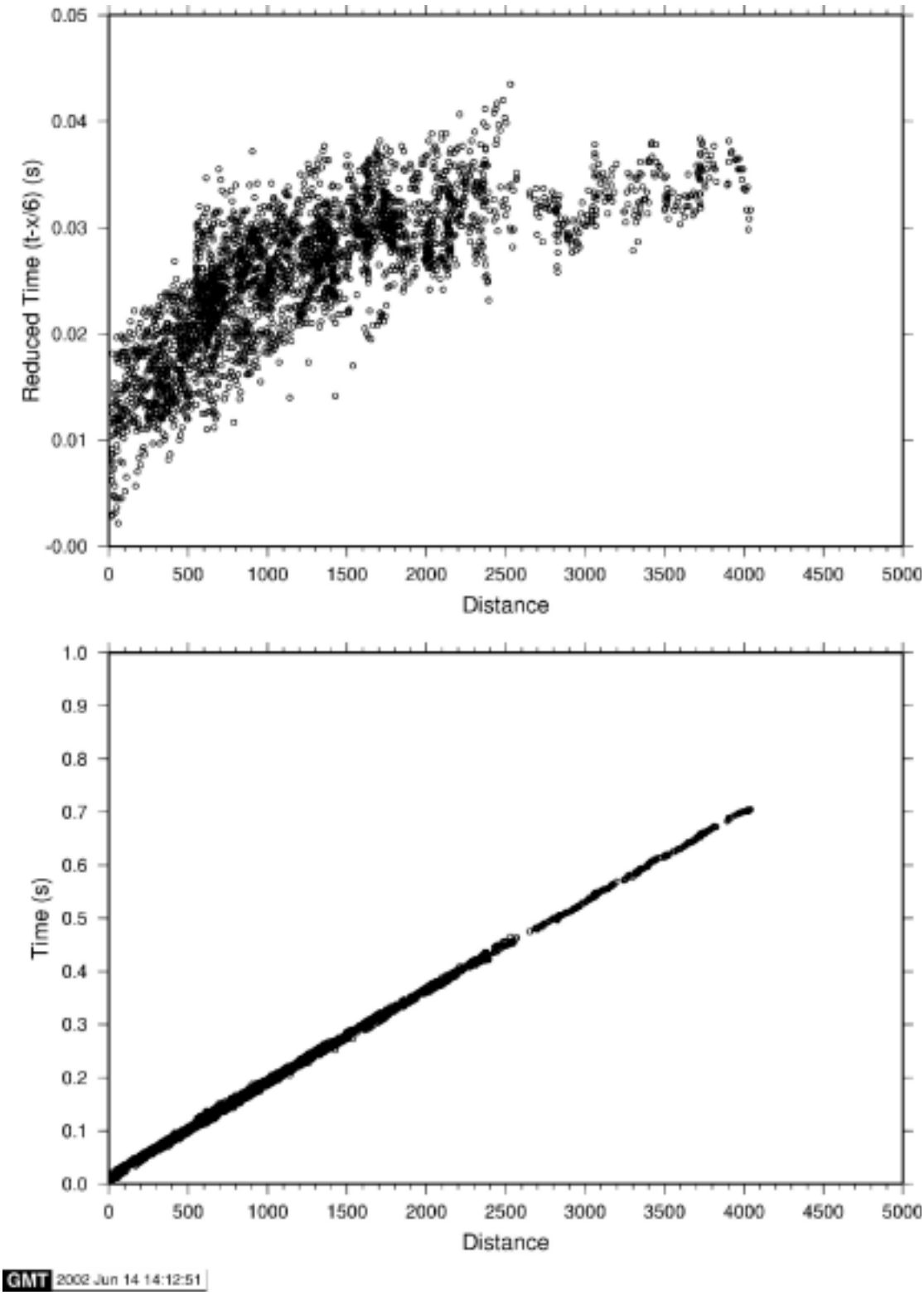


*Figure 3-15. Bottom - plot of all picked first breaks as a function of offset. Top -same data as bottom plot except that all picked first breaks have been reduced by 6000 m/s. After reducing the first breaks it is clear that a velocity gradient is present in the area.*

# 4. Interpretation

## 4.1. Reflection seismic

### *4.1.1. Background*

An important aspect of high-resolution seismic studies for nuclear waste disposal is the three dimensional imaging of reflectors and their correlation with borehole data. Fracture zone geometry is often complex and highly three dimensional (Tirén et al., 1999). Ideally, 3D data should be acquired, but this is a very expensive solution. When only 2D data are available, it is only in the vicinity of crossing lines that it is possible to calculate the true strike and dip of reflectors. Also, if reflections project to the surface on single-line data and can be correlated with a surface feature at the intersection point, then an estimate of the strike and dip can also be made.

Inspection of the stacked sections (Figures 3-3 to 3-13) shows the upper 3-4 km of crust to be highly reflective in parts of the Forsmark area. These reflections may be due to the presence of fracture zones, mafic sheets (sills or dikes), mylonite zones or lithological boundaries at depth. Experience has shown that mafic sheets, in particular, generate distinct high amplitude reflections. Reflections from fracture zones are generally weaker and less distinct. Lateral changes in the reflectivity along the profiles may be due to changes in the geology, but also to changes in acquisition conditions. Noise from the Forsmark power plant, crooked lines (Wu et al., 1995) and changes in the near surface conditions where the shots were fired may result in poorer images of reflections along some portions of the stacked sections.

### *4.1.2. General Observations*

The most prominent reflection or set of reflections on the sections is the one on profile 4 (Figure 3-9) with an apparent dip to the south. This 100 ms (300 m) wide band is observed between 0.8 to 0.9 s at the southern end of the profile, extends across the entire section, and is observed between 0.3 and 0.4 s on its northern end. On profile 1 (Figure 3-3) weaker sub-horizontal reflections are observed at about 0.5 to 0.6 s where it crosses profile 4. These reflections are, in all likelihood, coming from out-of-the-plane of the profile and originate from the same structure causing the prominent dipping set on profile 4. This implies that this structure dips at about 45° and strikes at approximately 75°. This structure will be referred to as the A1 reflector in this report. The bottom of this c. 100 ms thick package of reflections is referred to as A0. The A1 reflector is projected to intersect the surface about 1 km north of the northern end of profile 4 and projects to a point at about 2 km depth where the profiles cross. Note that the reflecting structure has not been imaged below the crossing point. Profile 4 would have to be extended about 1 km to the south in order to do this.

The clearest reflections from the uppermost 1 km are observed on the southeastern half of profile 5 and on profile 3. Two prominent sets are observed, set A and set B. Set A has a similar strike to the prominent A1 reflector and the dips are in the 20-30° range. Set B is more N-S striking with dips in the 20-35° range. Set A can generally be traced to the surface on profiles 3 and 5 and the projection of the reflectors to the surface can be regarded as fairly reliable. There are number of reflections with similar orientation to that of set A on profiles 3 and 5, but none of these can be traced to the

surface and have not been picked. Set B consists of reflections that are generally stronger than set A, but cannot reliably be traced to the surface, except for reflector B1. Both these sets will be discussed in more detail later in the report.

There are 2 sub-horizontal structures that generate reflections that can be observed over nearly all of the profiles (Figures 3-3, 3-5, 3-7, 3-9 and 3-11). These will be referred to as the C1 and C2 reflectors. Reflections from these 10-20° dipping structures are generally observed between 0.8 to 1.2 s (about 3 km). Their large depth relative to the charge size used in the surveys makes it uncertain whether they have been imaged on all portions of the sections. Signal penetration may not have been deep enough along some portions of the profiles.

### *4.1.3. Seismic modeling and correlation between profiles*

In order to obtain 3D control in the upper 1.5 km where the profiles cross, a combination of correlation of reflections between the profiles (Figures 4-1 to 4-4) and seismic modeling (Ayarza et al., 2000) has been used. In principle, a reflection observed on one profile should be observed on a crossing profile at the crossing point at the same traveltime. This is not always the case on the present data set, especially for weaker reflections. Different reflections may have been enhanced in the processing on the different profiles. The crooked line acquisition may also result in destructive stacking of certain reflections, especially those coming from out-of-the-plane of the profile. Also, since numerous reflections are present on some parts of the profiles it can be difficult to uniquely identify one and the same reflection on two crossing profiles due to interference effects.

In order to orient reflectors, reflections that can be correlated where the profiles cross have been picked and grouped according to their strike and dip. This implies that some stronger reflections that are present only on single profiles have not been picked and, consequently, not oriented. Structures generating reflections are given in Table 4-1 and ranked according to the likelihood that the reflector would be encountered in a drilling operation. As a check on the picking and the orientation, reflections from these interfaces have been modeled (Figures 4-5 to 4-12), assuming that the interfaces are planes of infinite extent, and then compared with the observed data in order to obtain some idea of the lateral extent of the reflecting interfaces. When the reflection is not observed on the section or its position does not match that expected from the modeling, then the assumption of the reflector being an infinite plane has broken down. In Figures 4-5 to 4-12 reflections are labeled as defined in Table 4-1 and color coded according to their rank. Note again that the red, blue and green lines are not picked reflections, but indicate on the seismic sections where the reflectors given in Table 4-1 are expected to appear if they correspond to planes of infinite extent.

The set A reflectors discussed earlier project to the surface in the eastern and southeastern portion of the study area (Figure 4-13), except for the A0/A1 reflector which projects to the surface north of the study area. The exact location of where the top of the A1 reflector intersects the surface is not entirely constrained, however, if the reflector is plane it projects to the surface at coordinates x=1630.75 km, y=6701.60 km along the northward continuation of profile 4 (Figure 4-14). Its strike is based on the correlation of sub-horizontal reflections on the eastern half of profile 1 (Figure 4-5) and the presence of a southward dipping reflection on the northern part of profile 5 (Figure 4-6). If a W-E running strike is assumed for the reflector then the

match between modeling and observed reflections is much poorer on profile 5.

There are numerous reflections with similar orientation to the B set discussed earlier. The picking of set was based on identifying the uppermost reflection (B1) having the set B orientation and the lowermost one (B5) with this orientation. Three strong reflections in between have also been picked and are included in set B (B2,B3 and B4). Reflections B2 and B3 can be followed northwestwards along profile 5 and appear to extend across the entire profile with the same orientation. B4 and B5 cannot be traced further northwest than to about CDP 700 on profile 5. B4 may be present on profile 1 (Figure 4-10) and on profile 4 (Figure 4-9), but this is speculative.

The I1 reflector has a similar strike to that of set B (Figure 4-13), but dips much more steeply (Figure 4-12). Therefore, it is not included in set B. There are signs of additional reflections originating from interfaces with a similar orientation to that of I1, but none have been picked.

The image on the southwestern part (CDPs 1-300) on profile 2 is not as clear as on the southeastern part of profile 5 and all of profile 3. Whether this is due to near-surface conditions or to the crooked acquisition geometry is not clear at present. The apparent sub-horizontal orientation of the set A and set B reflections on this line (Figure 4-11) is consistent with the strike and dip estimates made on profiles 3 and 5. The high amplitude reflection at about 150 ms on profile 5 between CDPs 550 and 700 is clearly not planar (reflector F1 in Table 4-1 and Figure 4-11). It has been modeled as originating from an interface striking at 20° and dipping at 20°, an orientation similar to the set B reflectors.

Reflection E1 at 0.65 s (Figure 4-7) is nearly horizontal, but is limited in its lateral extent. Even though it reflects from a deep interface, about 2 km depth, it has been modeled to indicate structures with this orientation are present in the area.

There are several weak sub-horizontal reflections on profile 1 in the upper 0.5 s (Figure 3-4). Note that the stronger sub-horizontal reflections between 0.5 and 0.6 s on profile 1 originate from the A1 structure (Figure 4-9). Some of the weaker ones above 0.5 s can possibly be correlated to weak sub-horizontal reflections on profile 4 (Figure 4-9) implying that they originate from sub-horizontal structures. These are labeled as set G. A steeply dipping set of reflections appears to overlap this sub-horizontal set in the upper 0.3 s and is labeled set H. This set strikes at 123° and dips at 70°. Interfaces to these reflections may extend to the southeast and H1 reflections may be observed on profile 2 (Figure 4-7). A relatively clear reflection on profile 4 intersects the surface at about CDP 225, close to corehole KFM01. Profile 1 runs north of this point so the reflector cannot be oriented directly. However, the reflection correlates with the projection of both the B4 and A2 reflectors that we oriented on profiles 3 and 5.

Reflections originating from structures D1, D2 and D3 (Figures 4-5 to 4-8) are highly speculative and are discussed in more detail in section 4.1.6.2.

### *4.1.4. Reflections which cannot be oriented*

There are number of clear reflections that appear only on single profiles and, therefore, cannot be oriented. Examples of these are the strong X1 reflection on profile 1 and the dipping Y1 reflection (Figure 4-5).

### *4.1.5. Projection of reflectors to 500 m depth*

It is of interest to trace the reflectors from surface to depth. Figure 4-15 indicates where those reflectors shown intersecting the surface in Figure 4-13 would intersect a depth level of 500 m

**Table 4-1. Orientation of reflectors as determined from the surface seismic and shown in Figure 4-13. Distance refers to distance from the arbitrary origin (6699 km N,1633 km W) to the closest point on the reflector at the surface. Depth refers to depth below the surface at this origin. Strike is measured clockwise from north. Rank indicates how sure the observation of each reflection is on profiles that the reflection is observed on; 1 – definite, 2- probable, 3-possible.**

| *Reflector* | *Strike* | *Dip* | *Distance (m)* | *Depth (m)* | *Rank* | *Profiles observed on* |
|---|---|---|---|---|---|---|
| A1 | 75 | 45 | 3200 | | 1 | 1, 2?, 3?, 4, 5? |
| A2 | 80 | 22 | 790 | | 1 | 2, 3, 4?, 5 |
| A3 | 65 | 25 | -10 | | 1 | 2?, 3, 5 |
| A4 | 65 | 25 | -950 | | 1 | 3, 5 |
| A5 | 75 | 30 | -1450 | | 1 | 3, 5 |
| A6 | 75 | 30 | -1875 | | 1 | 3, 5? |
| B1 | 30 | 25 | -600 | | 1 | 3, 5 |
| B2 | 30 | 25 | 950 | | 1 | 2?, 3, 5 |
| B3 | 30 | 21 | 1750 | | 1 | 2?, 3, 4?, 5 |
| B4 | 50 | 28 | 1460 | | 1 | 2, 3, 4?,5 |
| B5 | 50 | 25 | 2600 | | 1 | 3, 4?, 5 |
| C1 | 15 | 20 | | 3300 | 1 | 1, 2, 3, 4, 5 |
| C2 | 355 | 10 | | 3300 | 1 | 1, 2, 3, 4, 5 |
| D1 | 320 | 65 | 2500 | | 3 | 2, 5? |
| D2 | 120 | 50 | 2500 | | 3 | 2, 5? |
| D3 | 320 | 65 | 3200 | | 3 | 2, 5? |
| E1 | 270 | 9 | | 2020 | 2 | 2, 5 |
| F1 | 20 | 20 | | 400 | 2 | 2, 5 |
| G1 | 180 | 3 | | 100 | 3 | 1, 4 |
| G2 | 180 | 3 | | 200 | 3 | 1, 4 |
| G3 | 0 | 2 | | 1120 | 3 | 1, 4 |
| G4 | 0 | 2 | | 1220 | 3 | 1, 4 |
| H1 | 123 | 70 | -150 | | 2 | 1, 2?, 4 |
| H2 | 123 | 70 | -50 | | 2 | 1, 2?, 4 |
| I1 | 30 | 70 | -1100 | | 2 | 3, 5 |

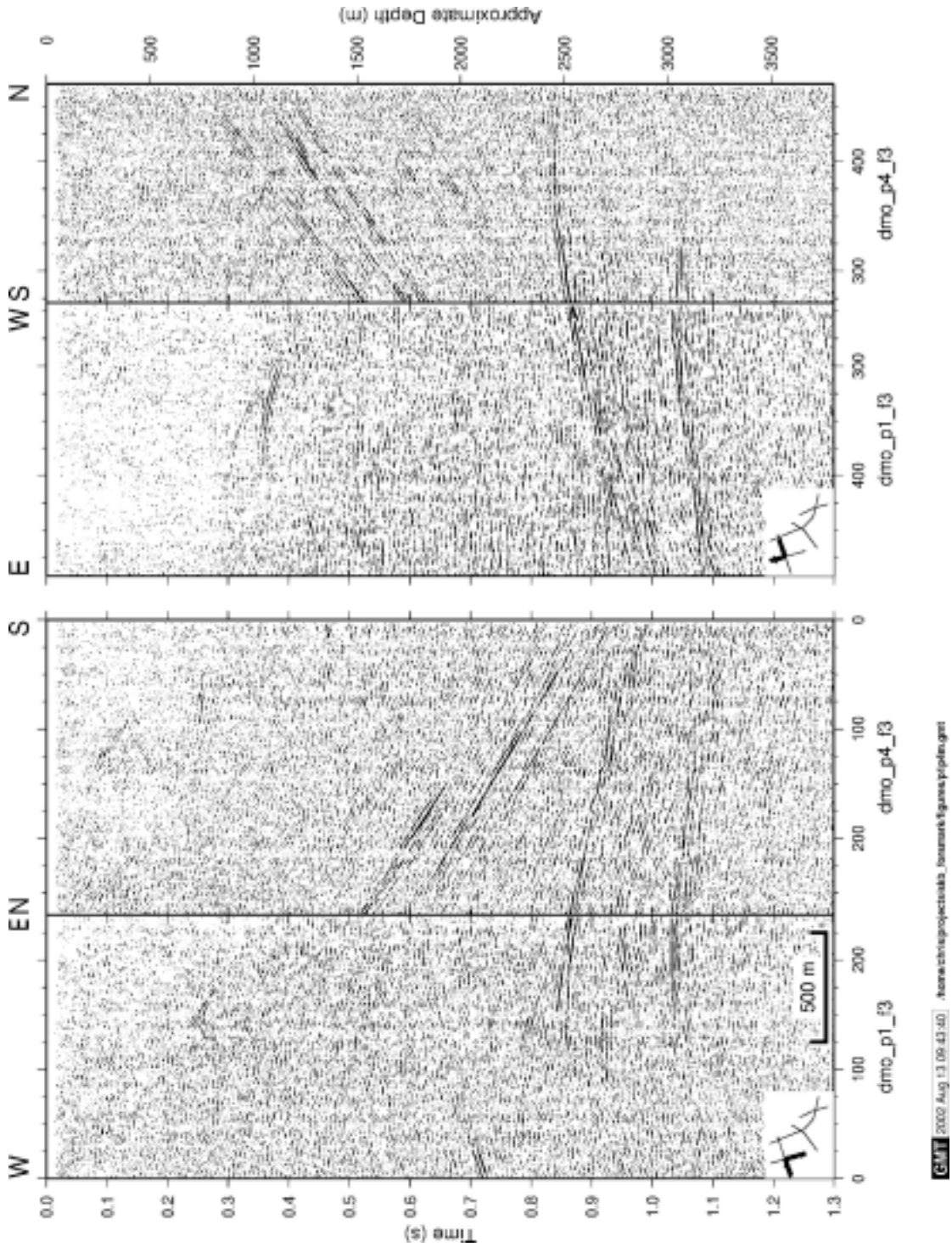


*Figure 4-1. Correlation of stacks from profiles 1 and 4 at their crossing point (Figure 3-1). Location of section indicated in lower left corner. Depth scale only valid for true sub-horizontal reflections. Horizontal numbering is CDP.*

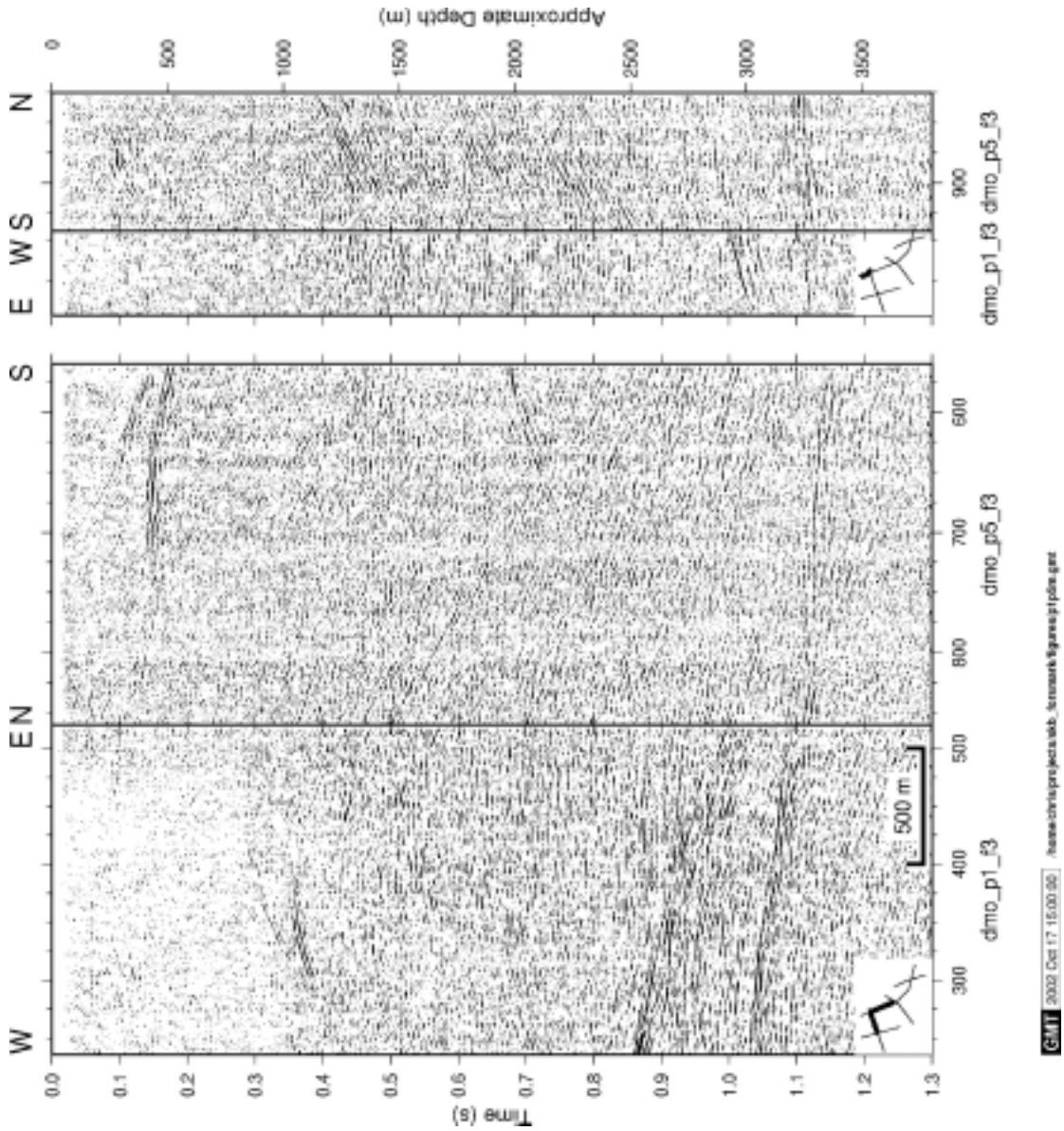


*Figure 4-2. Correlation of stacks from profiles 1 and 5 at their crossing point (Figure 3-1). Location of section indicated in lower left corner. Depth scale only valid for true sub-horizontal reflections. Horizontal numbering is CDP.*

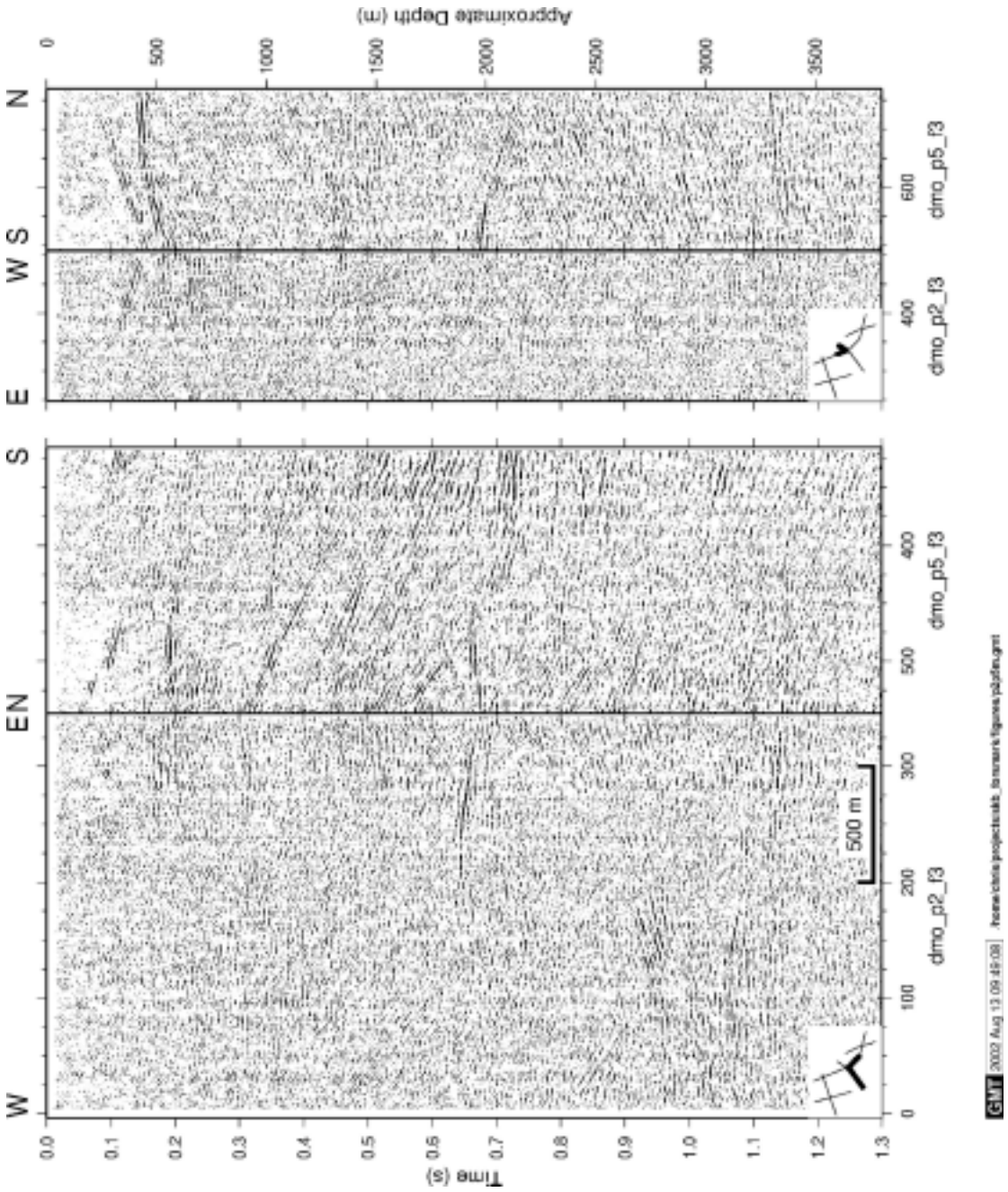


*Figure 4-3. Correlation of stacks from profiles 2 and 5 at their crossing point (Figure 3-1). Location of section indicated in lower left corner. Depth scale only valid for true sub-horizontal reflections. Horizontal numbering is CDP.*

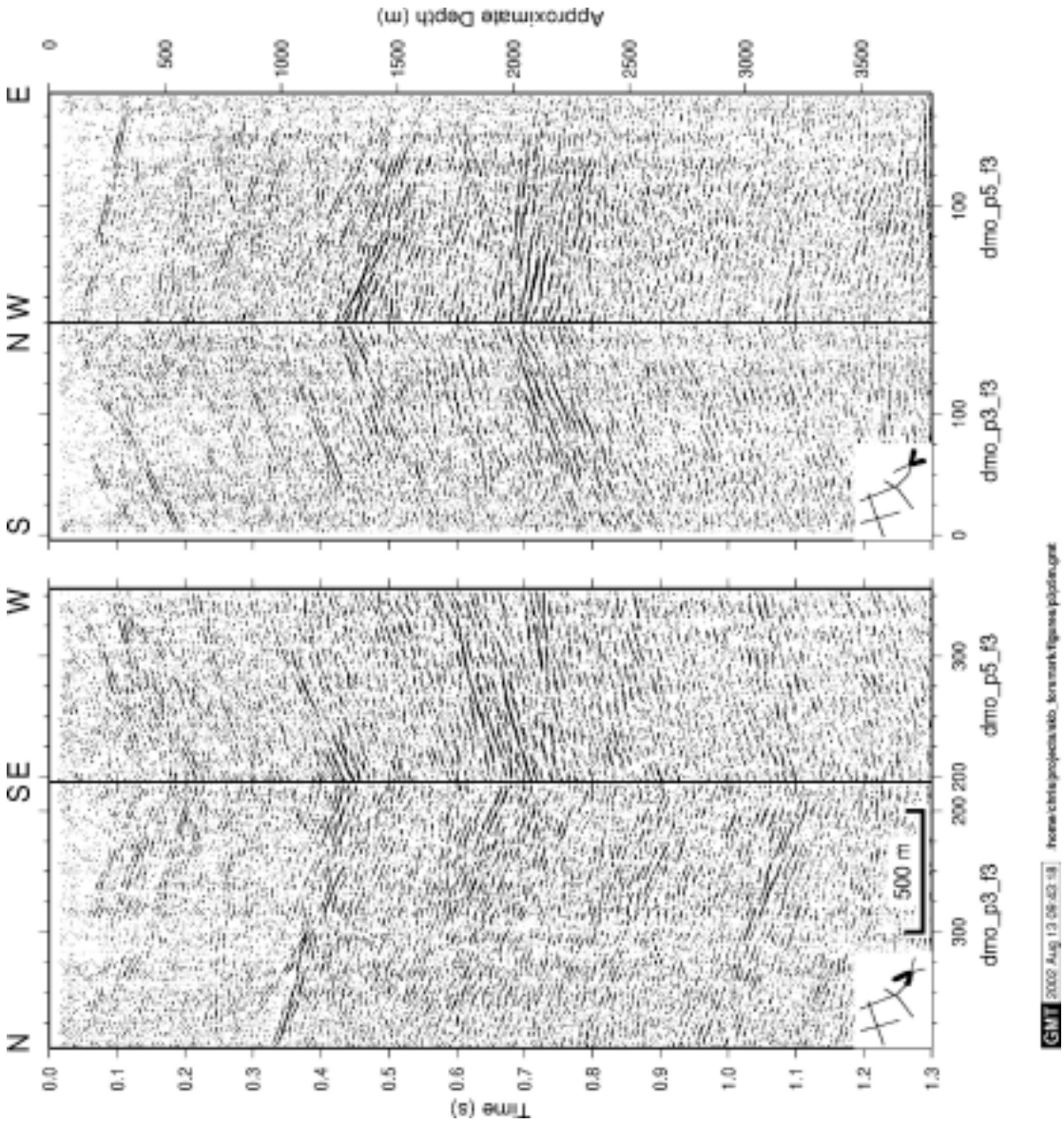


*Figure 4-4. Correlation of stacks from profiles 3 and 5 at their crossing point (Figure 3-1). Location of section indicated in lower left corner. Depth scale only valid for true sub-horizontal reflections. Horizontal numbering is CDP.*

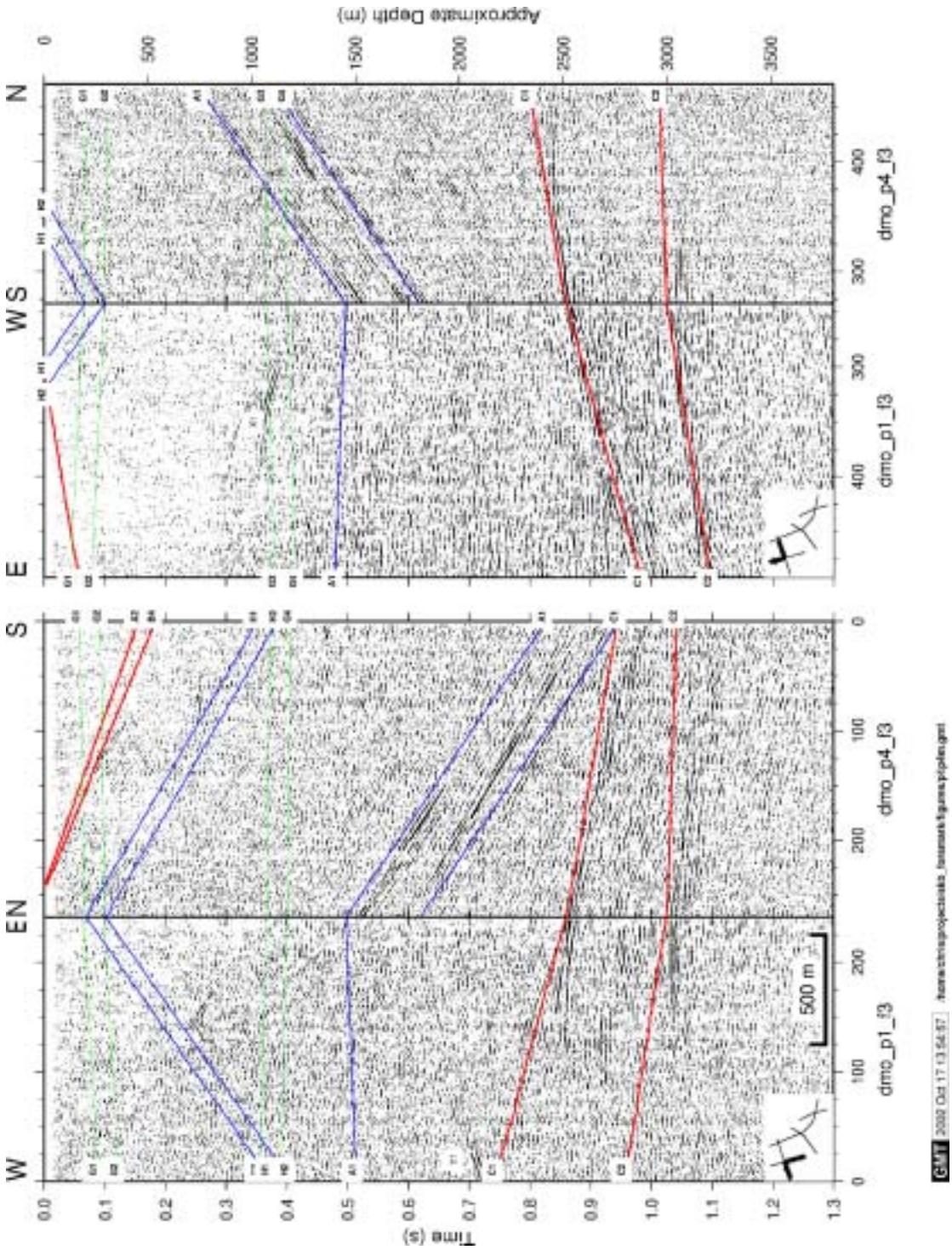


*Figure 4-5. Correlation of stacks from profiles 1 and 4 at their crossing point (Figure 3-1) and comparison with modeling the reflectors defined in Table 4-1. Modeling of reflectors is coded as follows: red-rank 1, blue-rank 2, green-rank 3. Note that these lines are where reflections are expected to be observed on the seismic sections based on the strike and dips given in Table 4-1, they are* ***not*** *picked reflections. Location of section indicated in lower left corner. Depth scale only valid for true sub-horizontal reflections. Horizontal numbering is CDP.*

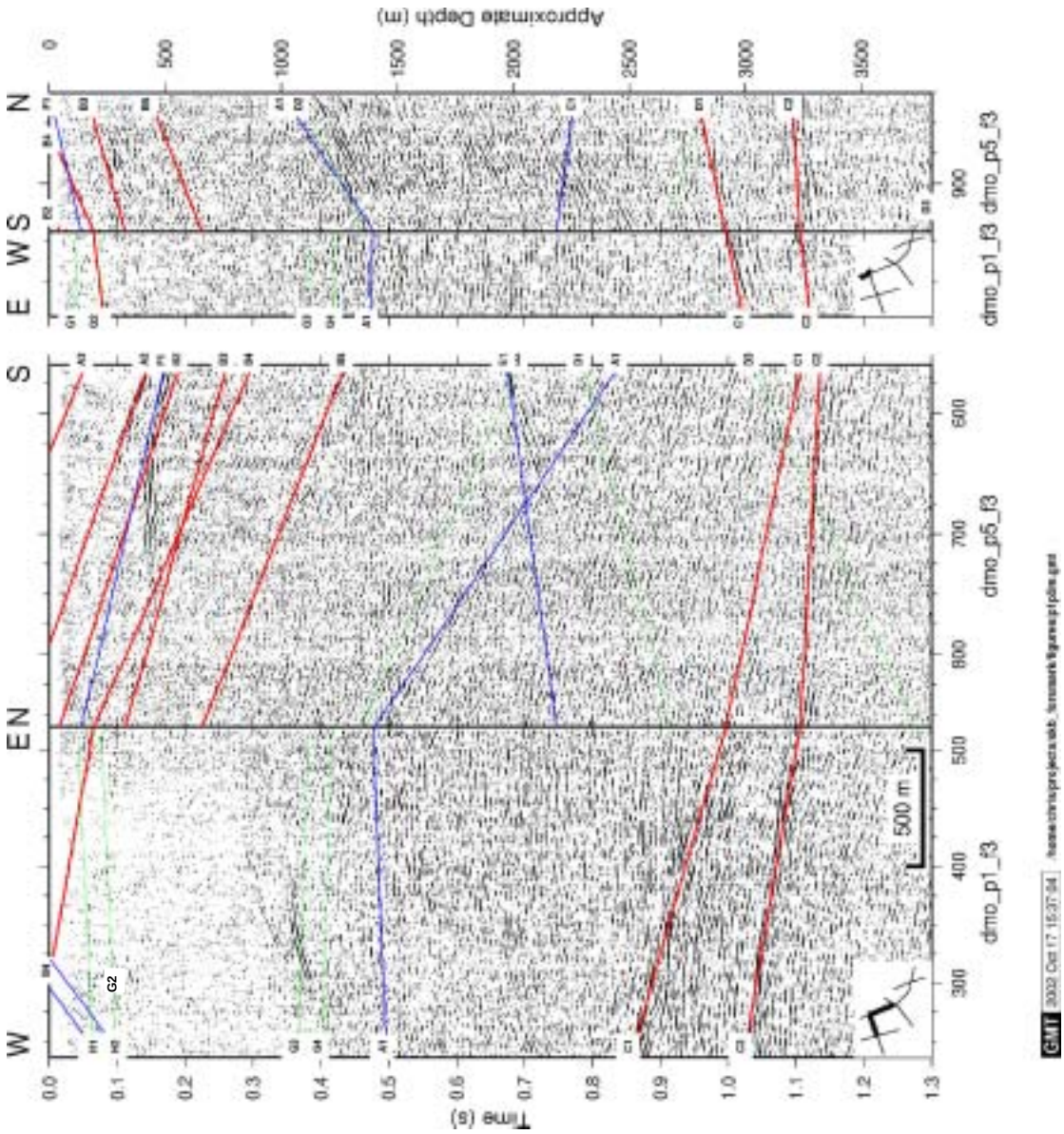


*Figure 4-6. Correlation of stacks from profiles 1 and 5 at their crossing point (Figure 3-1) and comparison with modeling the reflectors defined in Table 4-1. Modeling of reflectors is coded as follows: red-rank 1, blue-rank 2, green-rank 3. Note that these lines are where reflections are expected to be observed on the seismic sections based on the strike and dips given in Table 4-1, they are* ***not*** *picked reflections. Location of section indicated in lower left corner. Depth scale only valid for true sub-horizontal reflections. Horizontal numbering is CDP.*

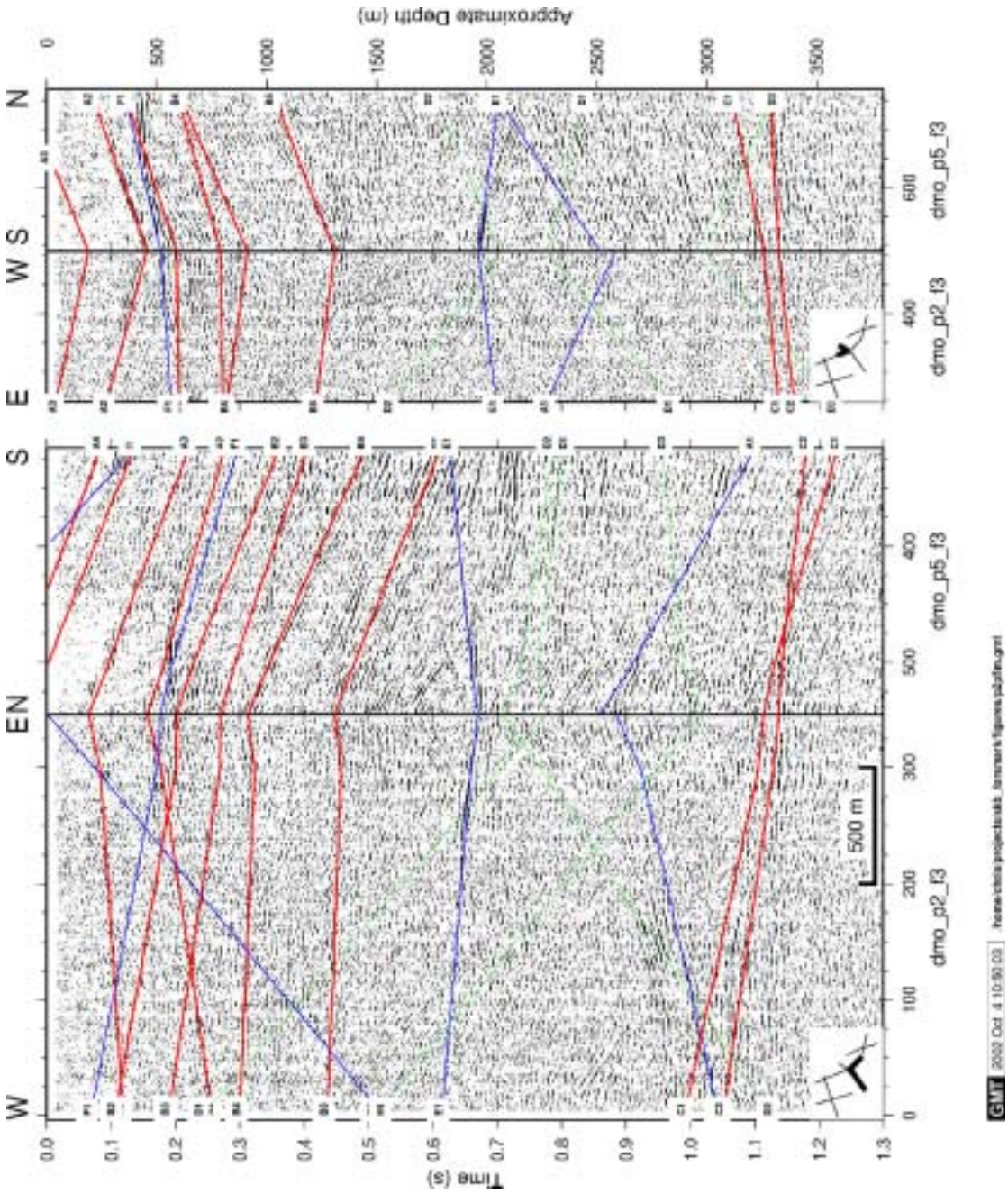


*Figure 4-7. Correlation of stacks from profiles 2 and 5 at their crossing point (Figure 3-1) and comparison with modeling the reflectors defined in Table 4-1. Modeling of reflectors is coded as follows: red-rank 1, blue-rank 2, green-rank 3. Note that these lines are where reflections are expected to be observed on the seismic sections based on the strike and dips given in Table 4-1, they are* ***not*** *picked reflections. Location of section indicated in lower left corner. Depth scale only valid for true sub-horizontal reflections. Horizontal numbering is CDP.*

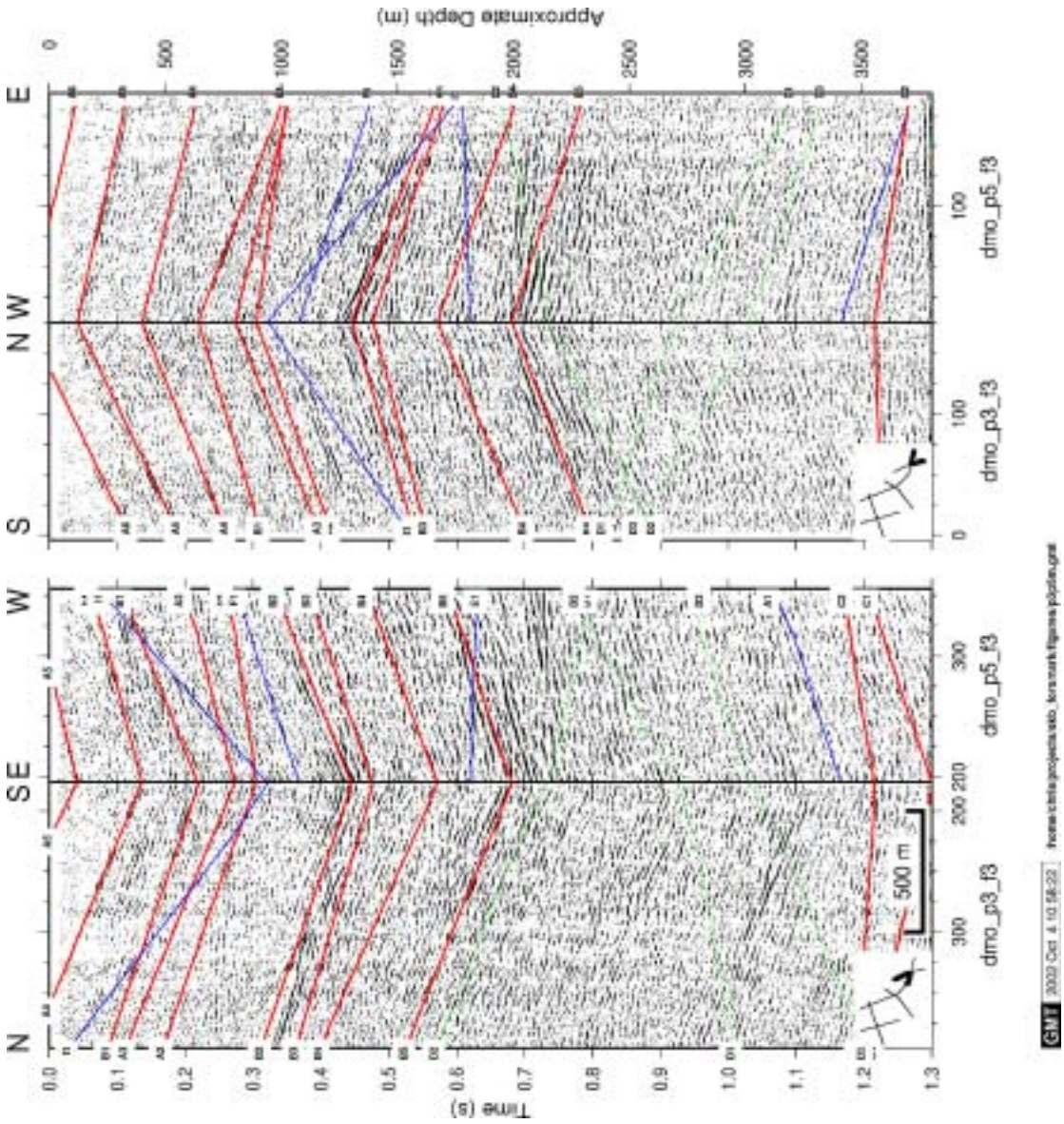


*Figure 4-8. Correlation of stacks from profiles 3 and 5 at their crossing point (Figure 3-1) and comparison with modeling the reflectors defined in Table 4-1. Modeling of reflectors is coded as follows: red-rank 1, blue-rank 2, green-rank 3. Note that these lines are where reflections are expected to be observed on the seismic sections based on the strike and dips given in Table 4-1, they are* ***not*** *picked reflections. Location of section indicated in lower left corner. Depth scale only valid for true sub-horizontal reflections. Horizontal numbering is CDP.*

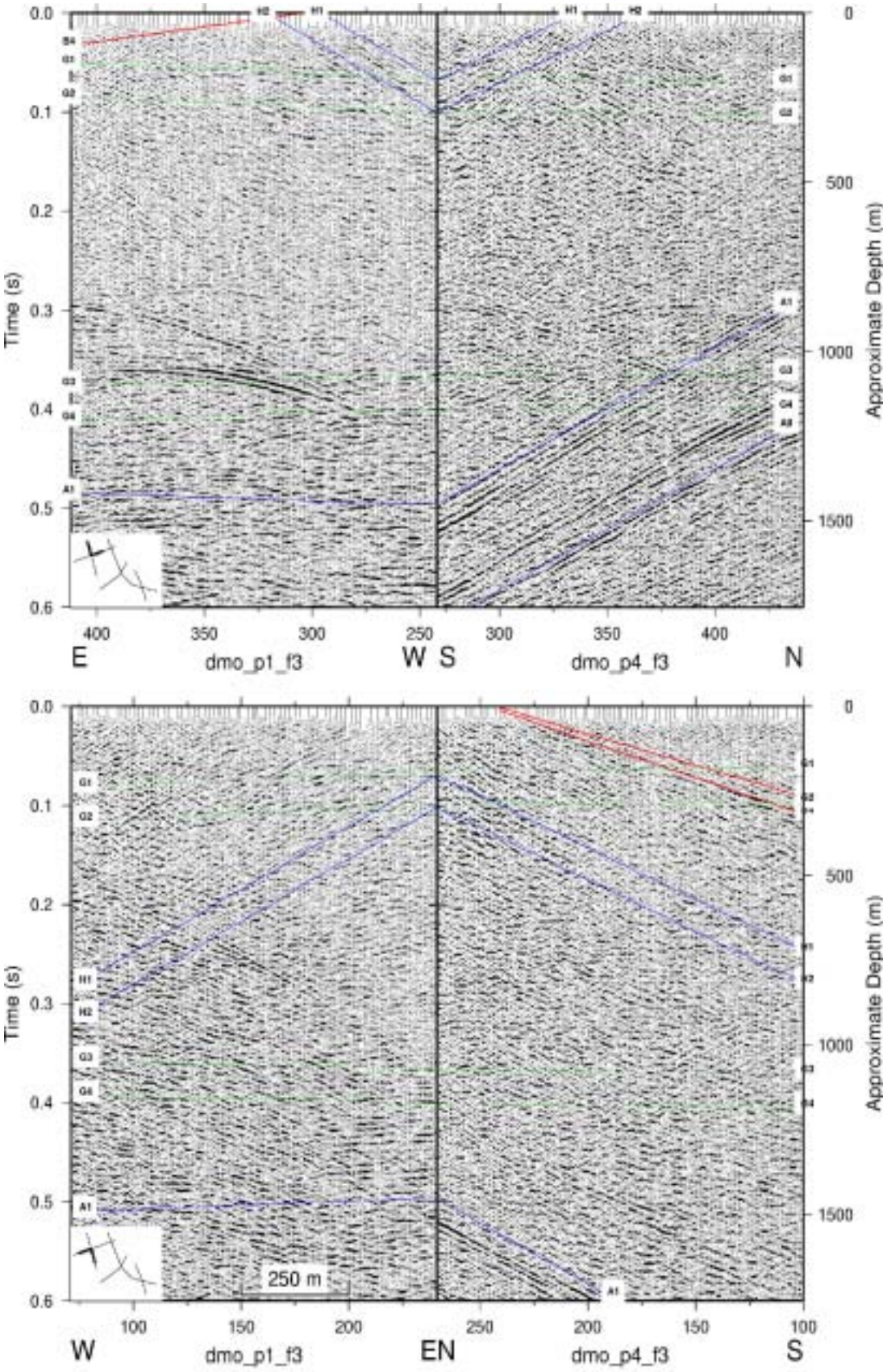


*Figure 4-9. Detailed correlation of stacks from profiles 1 and 4 at their crossing point (Figure 3-1) and comparison with modeling the reflectors defined in Table 4-1. Location of section indicated in lower left corner. Depth scale only valid for true sub-horizontal reflections.*

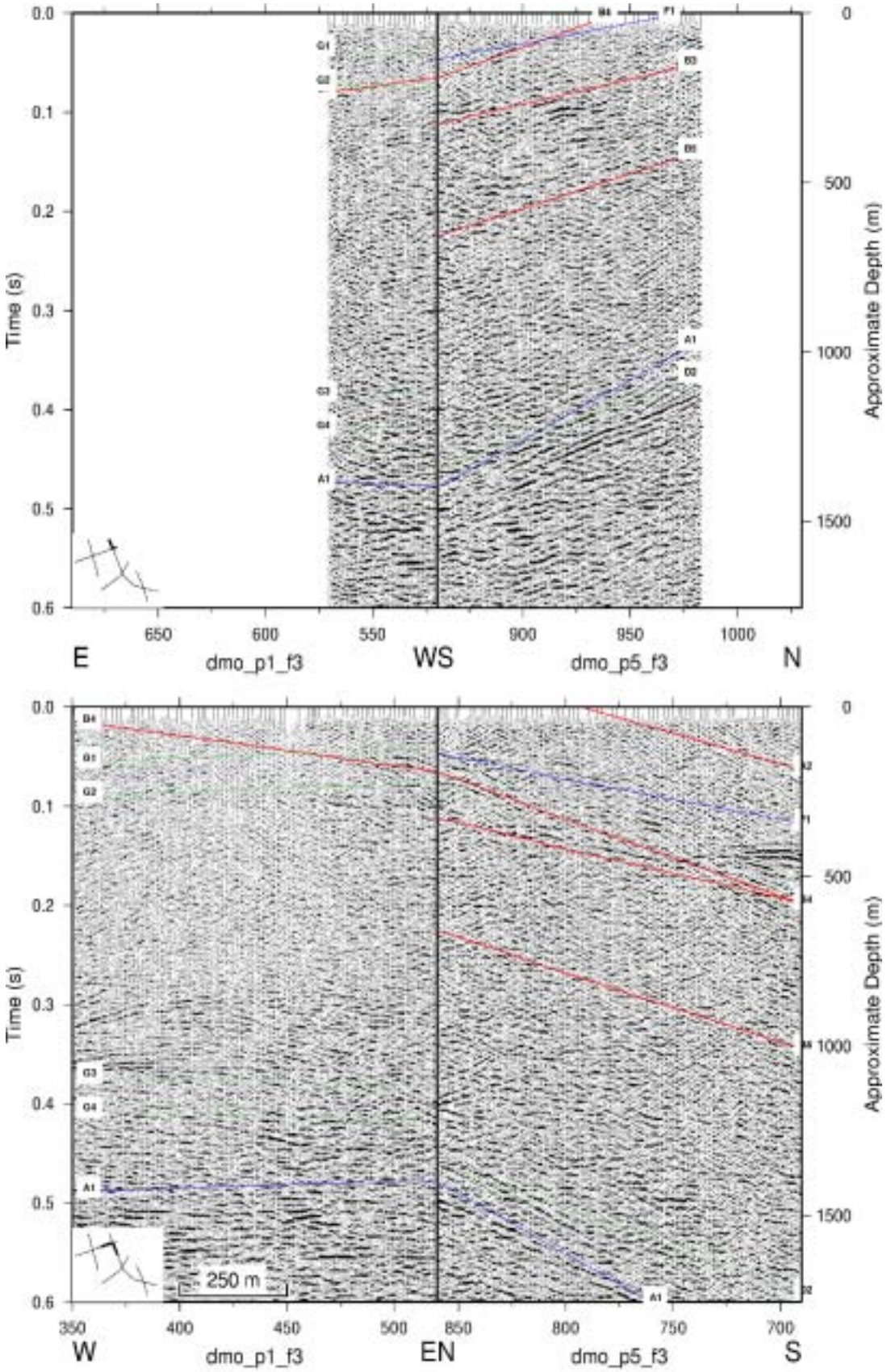


*Figure 4-10. Detailed correlation of stacks from profiles 1 and 5 at their crossing point (Figure 3-1) and comparison with modeling the reflectors defined in Table 4-1. Location of section indicated in lower left corner. Depth scale only valid for true sub-horizontal reflections.*

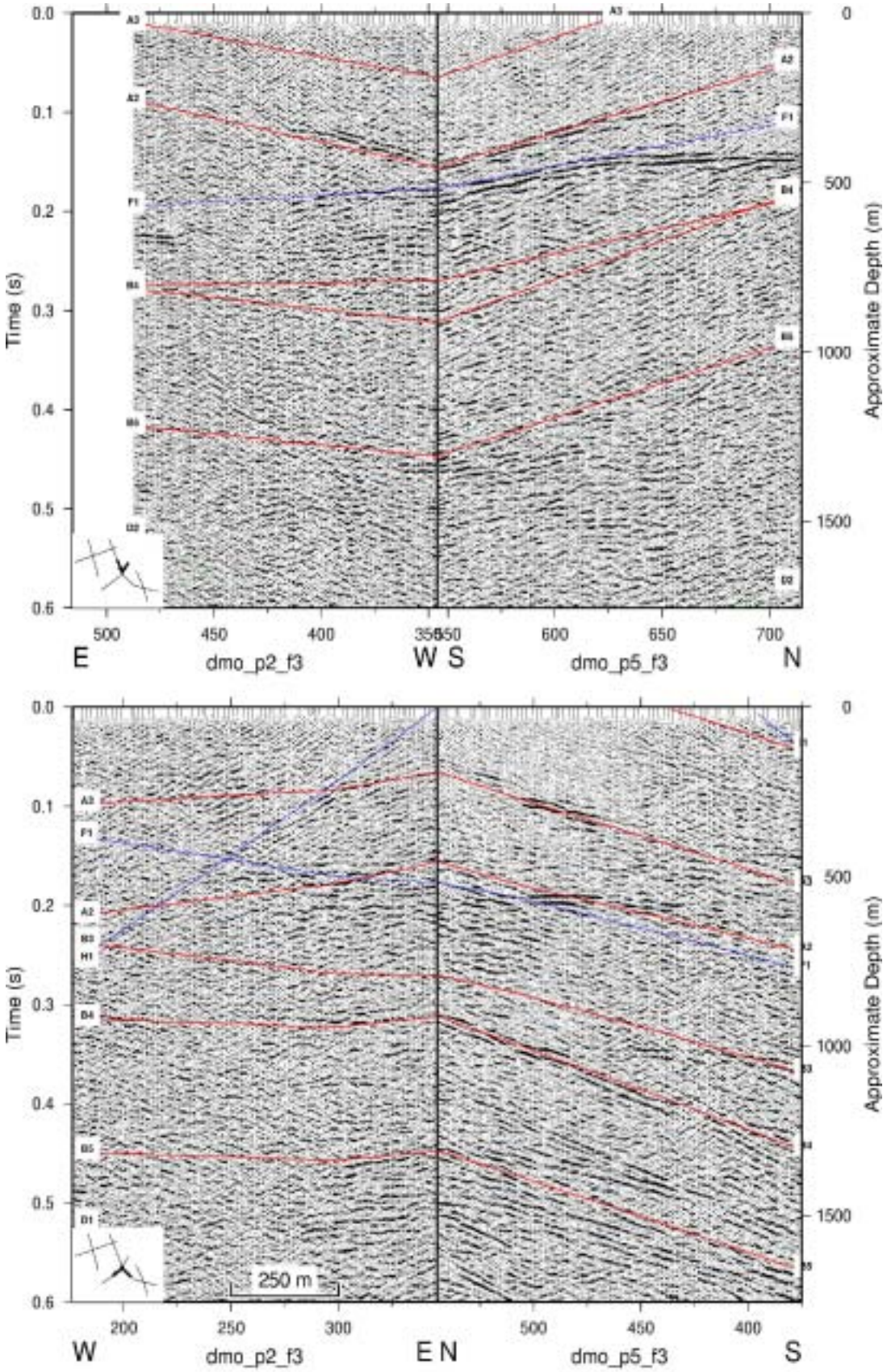


*Figure 4-11. Detailed correlation of stacks from profiles 2 and 5 at their crossing point (Figure 3-1) and comparison with modeling the reflectors defined in Table 4-1. Location of section indicated in lower left corner. Depth scale only valid for true sub-horizontal reflections.*

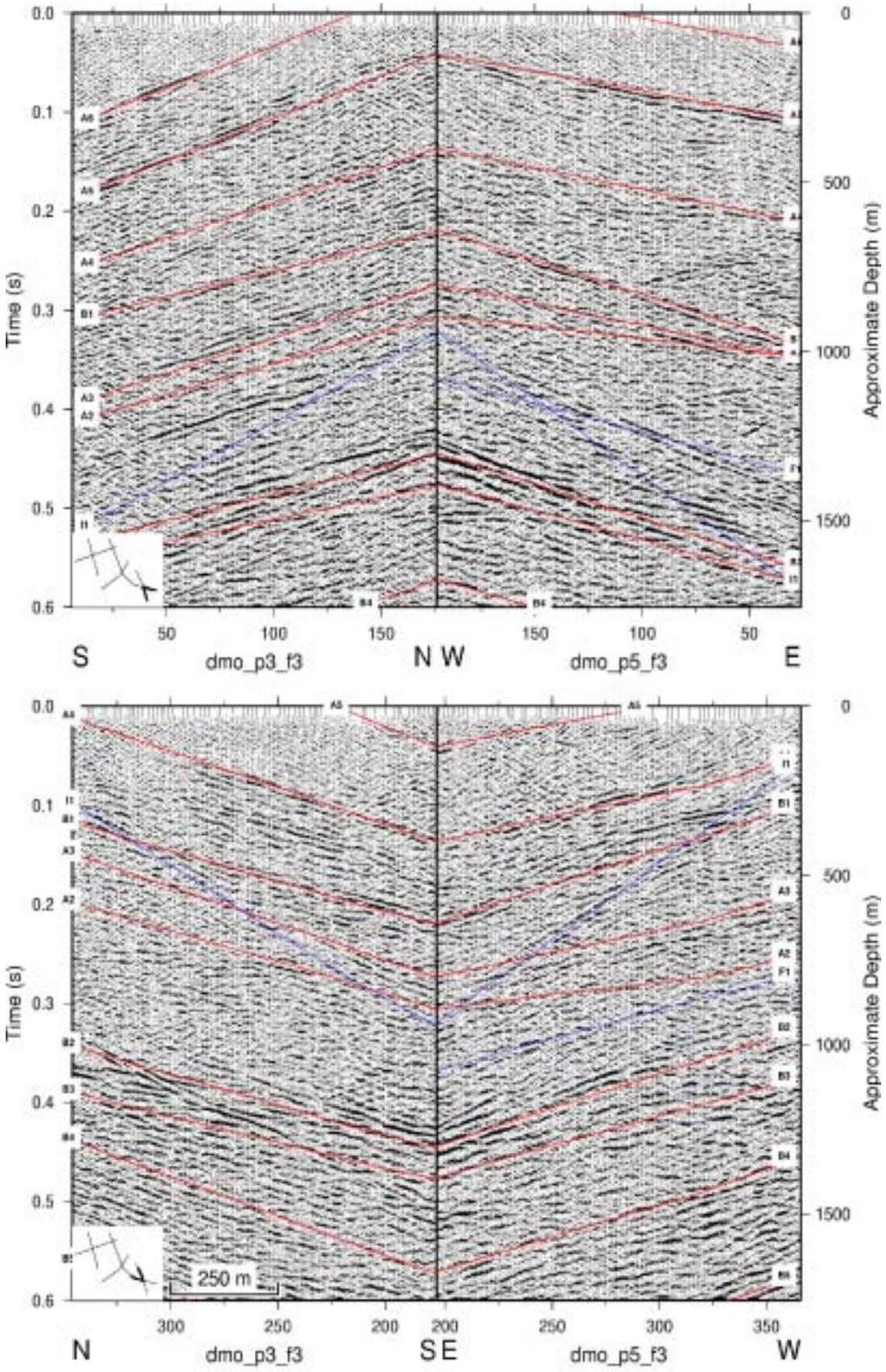


*Figure 4-12. Detailed correlation of stacks from profiles 3 and 5 at their crossing point (Figure 3-1) and comparison with modeling the reflectors defined in Table 4-1. Location of section indicated in lower left corner. Depth scale only valid for true sub-horizontal reflections.*

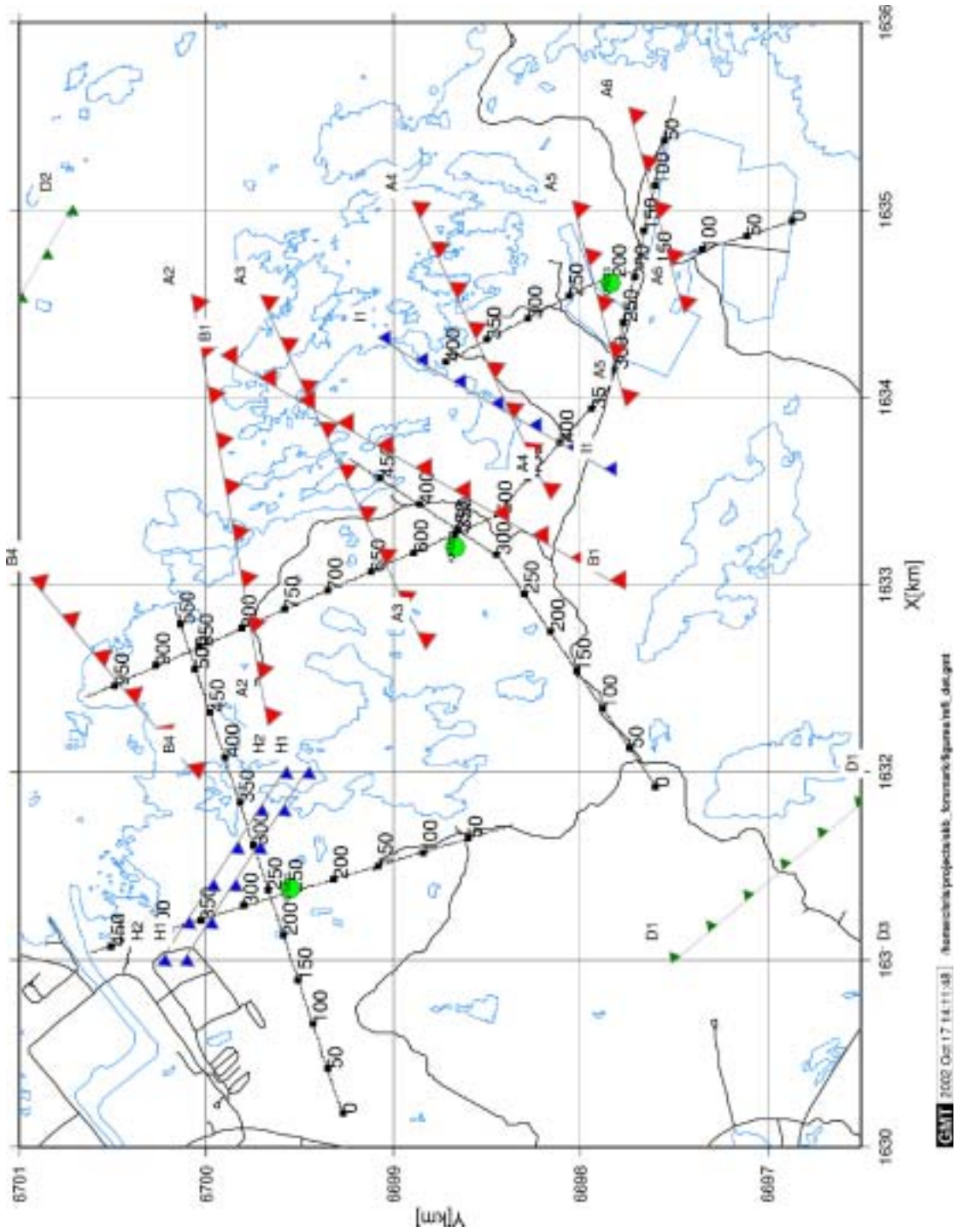


*Figure 4-13. Projected reflector intersections with the surface for those reflectors which project up to the surface in the Forsmark area. Reflections from interfaces that clearly cannot be traced to the surface, such as F1 in Table 4-1, are not drawn. Picked reflectors correspond to the tops of the reflector. Reflectors are coded as follows: red-rank 1, blue-rank 2, green-rank 3. Location of the first three planned deep borehole shown as green circles.*

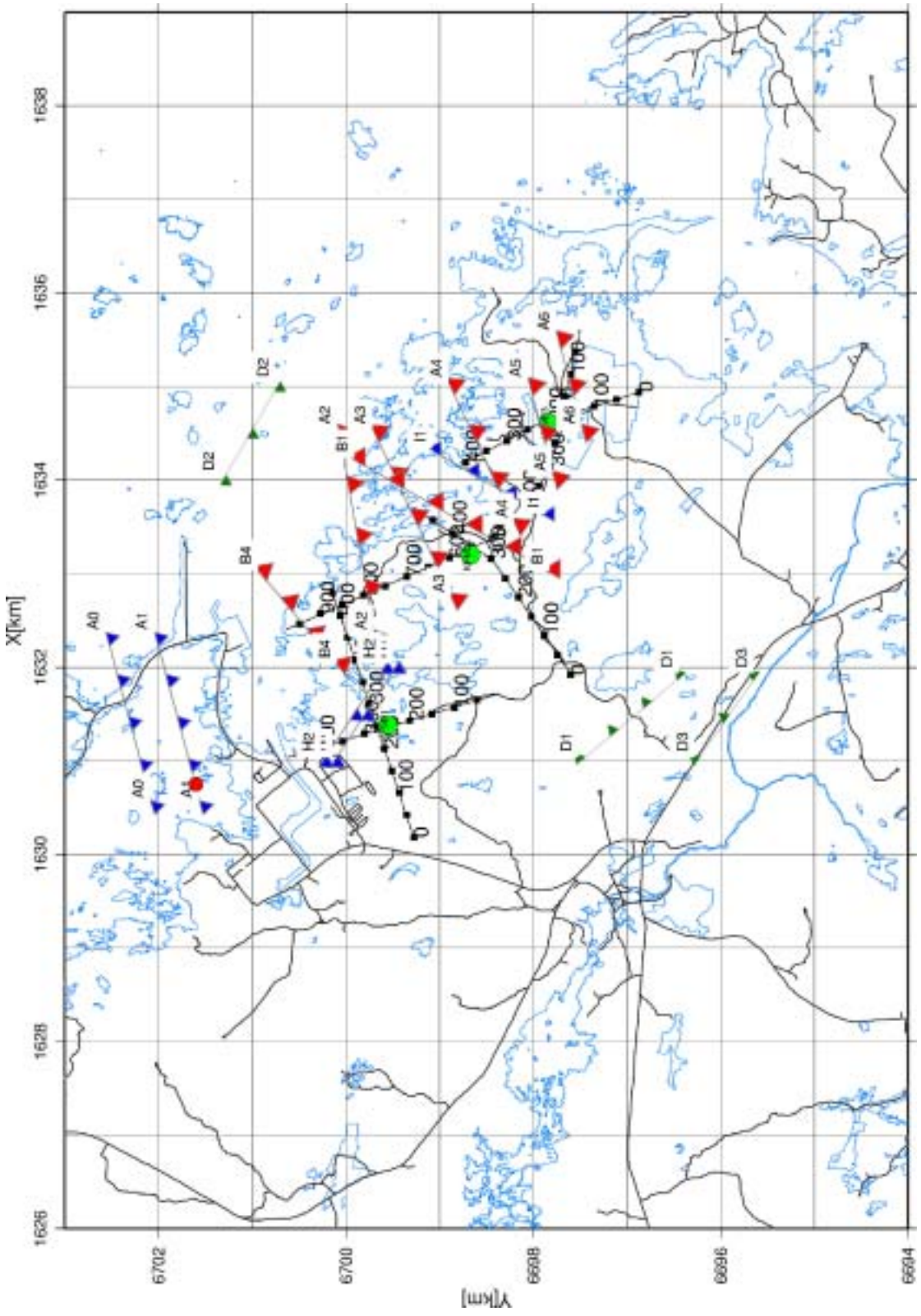


*Figure 4-14. As Figure 4-13, but covering a larger area. Picked reflectors correspond to the tops of the reflector. Reflectors are coded as follows: red-rank 1, blue-rank 2, green-rank 3. The red dot on the A1 reflector marks the point where this reflector would intersect the surface along the northward continuation of profile 4 if it is plane. The A0 reflector represents the base of the A1 reflection package, thus giving an indication of where this package may be expected to be observed at the surface. Location of the first three planned deep borehole shown as green circles.*

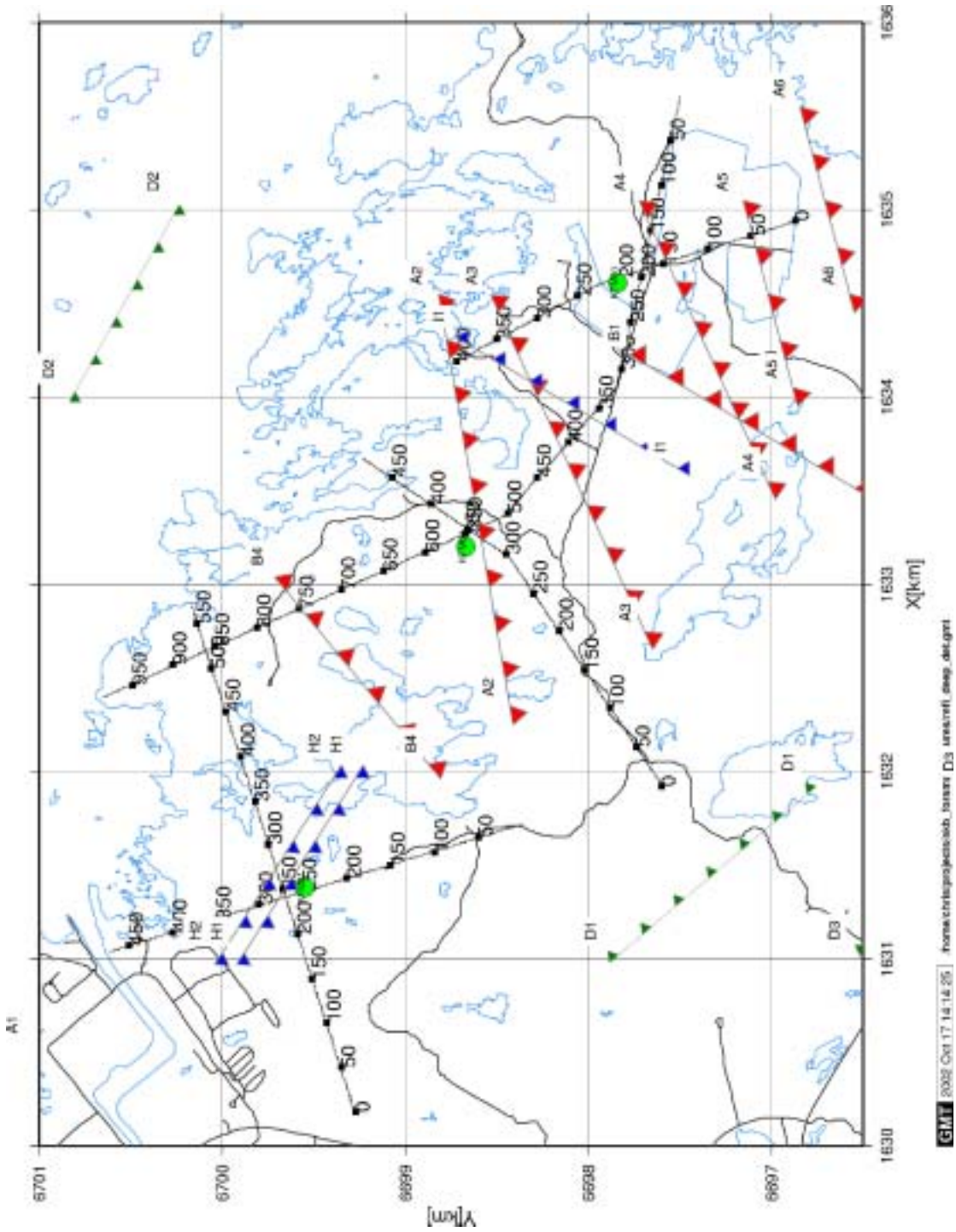


*Figure 4-15. Projected reflector intersections with a depth of 500 m for those reflectors which project up to the surface in the Forsmark area. Reflections from interfaces that clearly cannot be traced to the surface, such as F1 in Table 4-1, are not drawn. Picked reflectors correspond to the tops of the reflector. Reflectors are coded as follows: red-rank 1, blue-rank 2, green-rank 3. Location of the first three planned deep borehole shown as green circles.*

### 4.1.6. Correlation with surface data

#### 4.1.6.1 Topography

There is a tendency for the set A and some of the set B reflectors (B1 and possibly B2 and B4) to project to the surface in the vicinity of topographic anomalies (Figure 4-16). In general, topographic highs exist on the downdip side of the reflectors, even reflector I1 is associated with a topographic high on its downdip side.

#### 4.1.6.2 Magnetics

Reflectors D1, D2 and D3 are speculative. Signs of these reflectors are found primarily on profile 2. These reflections project up to the surface in the vicinity of magnetic linear lows (Figure 4-17). Reflections from D3 also project to the surface where there is a break in the topography (Figure 4-16). In order to verify that these reflections originate from structures associated with the magnetic lows the profiles need to be extended to cross these lows. It is possible that much stronger reflections are generated from structures dipping in the opposite direction to the potential D1, D2 and D3 reflectors or that the magnetic lows correspond to near-vertical structures.

The interpreted N75E striking A1 reflector (as projected to the surface) tends to follow a similar striking magnetic low(Figure 4-17) suggesting that the two are related.

#### 4.1.6.3 Infrared image

Projection of the reflectors to the surface on an infrared image (Figure 4-18) shows the same trend for the set A and some the set B reflectors as in the topography (Figure 4-16).

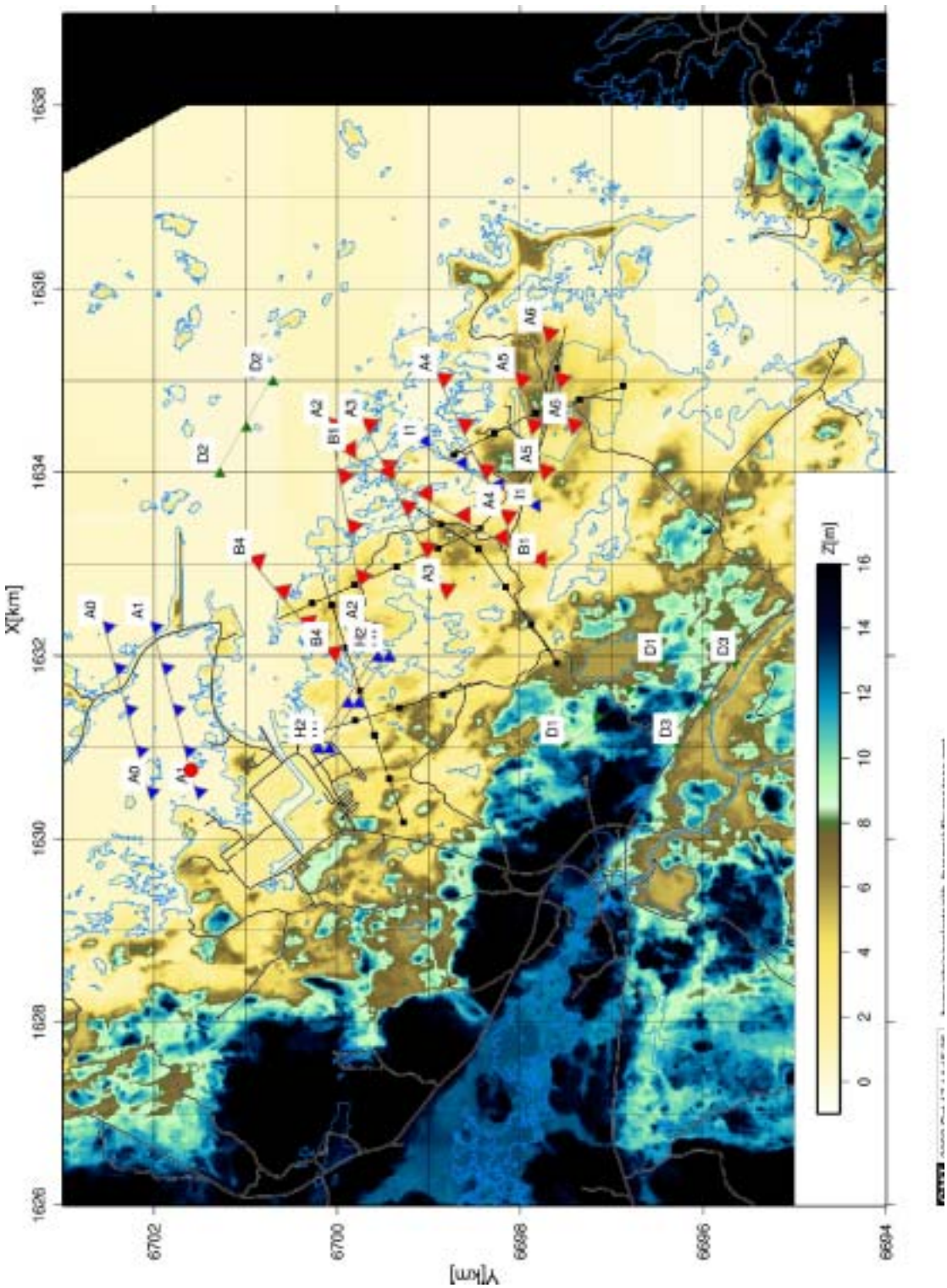


*Figure 4-16. Projected reflector intersections with the surface plotted on the topographic map. Reflections from interfaces that clearly cannot be traced to the surface, such as F1 in Table 4-1, are not drawn. All indicated reflectors correspond to relatively thin zones (5-15 m thick), except for the A1 reflector which is about 300 m thick. The bottom of this zone is indicated by the A0 reflector. Reflectors are coded as follows: red-rank 1, blue-rank 2, green-rank 3.*

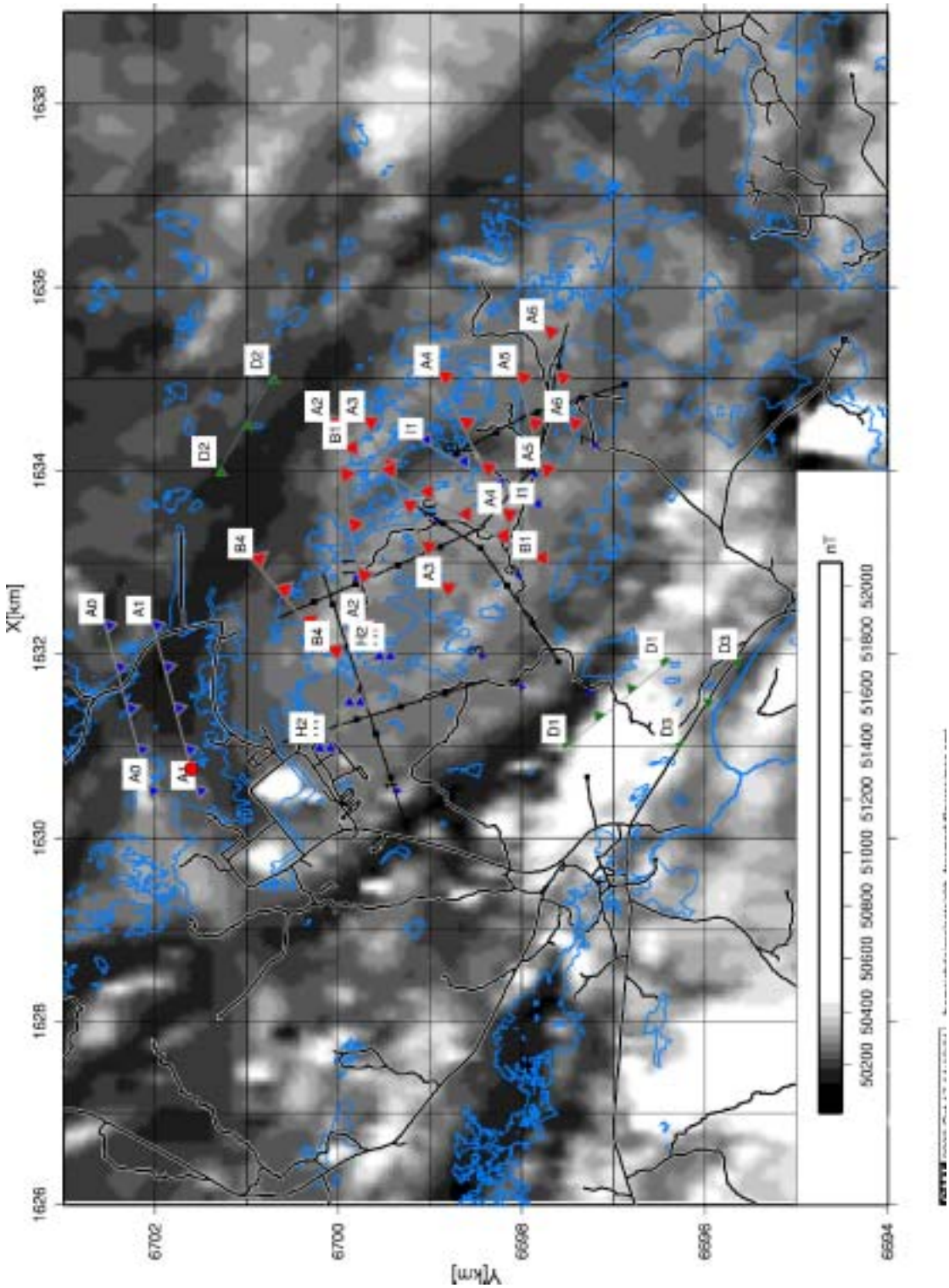


*Figure 4-17. Projected reflector intersections with the surface plotted on the total field magnetic map. Reflections from interfaces that clearly cannot be traced to the surface, such as F1 in Table 4-1, are not drawn. All indicated reflectors correspond to relatively thin zones (5-15 m thick), except for the A1 reflector which is about 300 m thick. The bottom of this zone is indicated by the A0 reflector. Reflectors are coded as follows: red-rank 1, blue-rank 2, green-rank 3.*

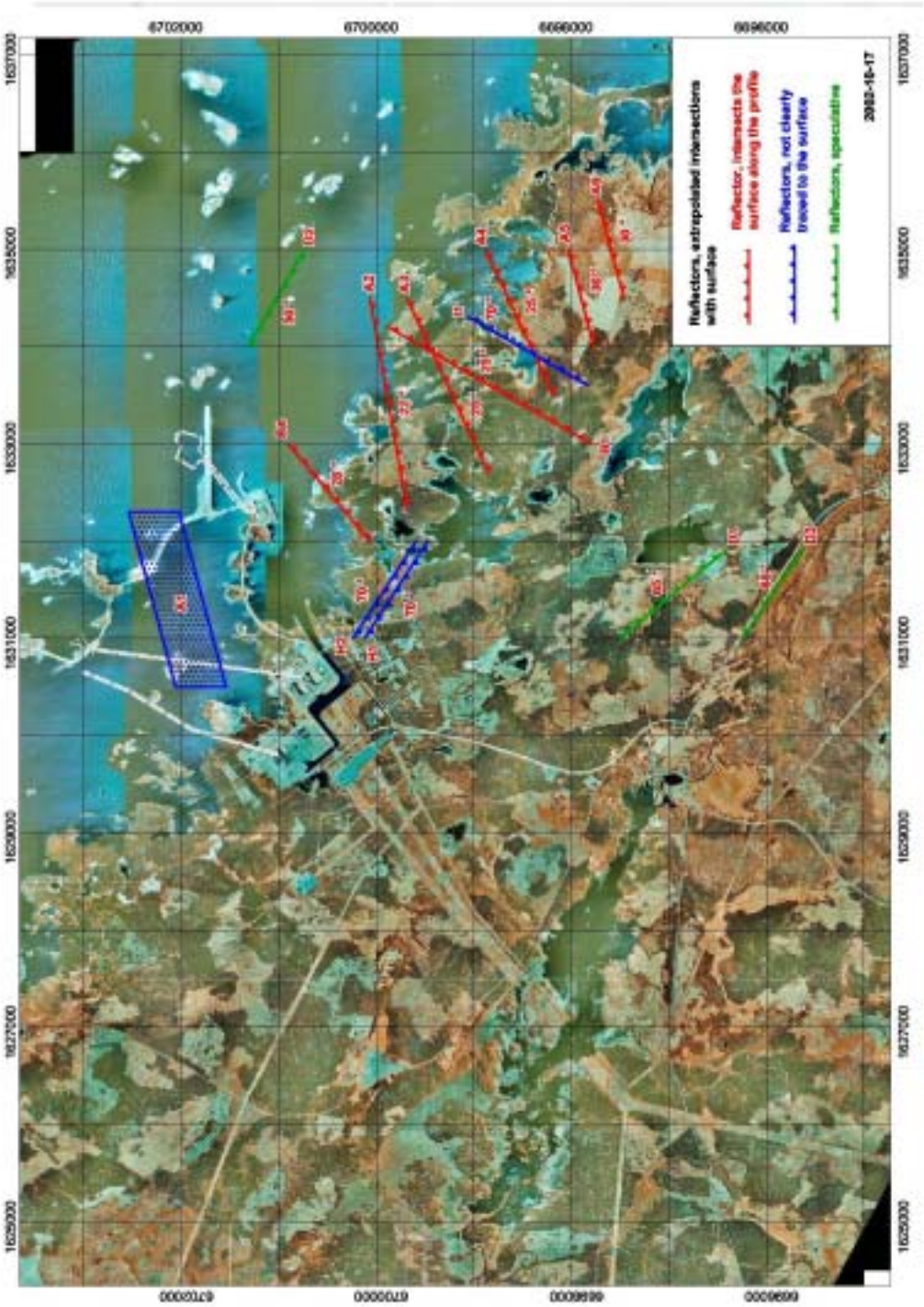


*Figure 4-18. Reflectors plotted on an infrared image. Reflections from interfaces that clearly cannot be traced to the surface, such as F1 in Table 4-1, are not drawn. All indicated reflectors correspond to relatively thin zones (5-15 m thick), except for the A1 reflector which is about 300 m thick. The bottom of this zone is indicated by the A0 reflector. Reflectors are coded as follows: red-rank 1, blue-rank 2, green-rank 3.*

## 4.2. Orion stations

Determination of the velocity field of an area is important for two reasons. First, the velocity field is used to convert time to depth. Without a proper estimate of the velocity field the depths to reflectors cannot be estimated accurately. Secondly, variations in the velocity field can provide structural information.

A preliminary 1D velocity model for the Forsmark area based on the Orion first arrival traveltimes is shown in Figure 4-19. This velocity model was the starting point for estimating 3D velocity models using a LSQR based inversion code (Benz et al, 1996; Tryggvason et al., 2002). An initial 3D model is determined by using the differences between predicted traveltimes through the 1D model and observed traveltimes. Once a satisfactory initial 3D model is obtained (Figure 4-20), the model is refined by repeating the inversion procedure to produce updated 3D velocity models (Figure 4-21). Results after 10 iterations of this procedure are shown in Figure 4-22 and Figure 4-23. The most prominent feature on the plan view (Figure 4-22) is a low velocity zone running in the NW-SE direction sub-parallel to profile AA'. This low velocity zone does not appear to extend far below 200 m depth as seen in in the section along profile BB' (Figure 4-23), but this may be an artifact of the acquisition geometry.

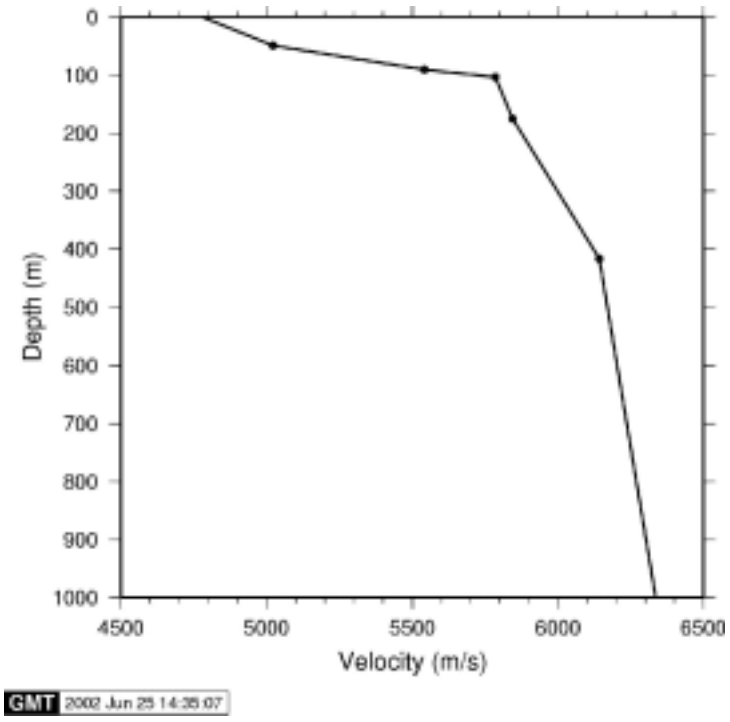


*Figure 4-19. Initial 1D P-wave velocity model for the Forsmark area based on first arrival times from the Orion stations.*

Clear reflections are observed in the Orion station data. Many of these reflections originate from the same reflectors as listed in Table 4-1. For example, modeling of the set B reflections produces synthetic seismograms which qualitatively match the real data on the southern part of profile 5 (compare Figure 4-24 with Figure 3-14). However, this match is not unique, and some of the reflections may also be qualitatively matched by modeling the set A reflectors.

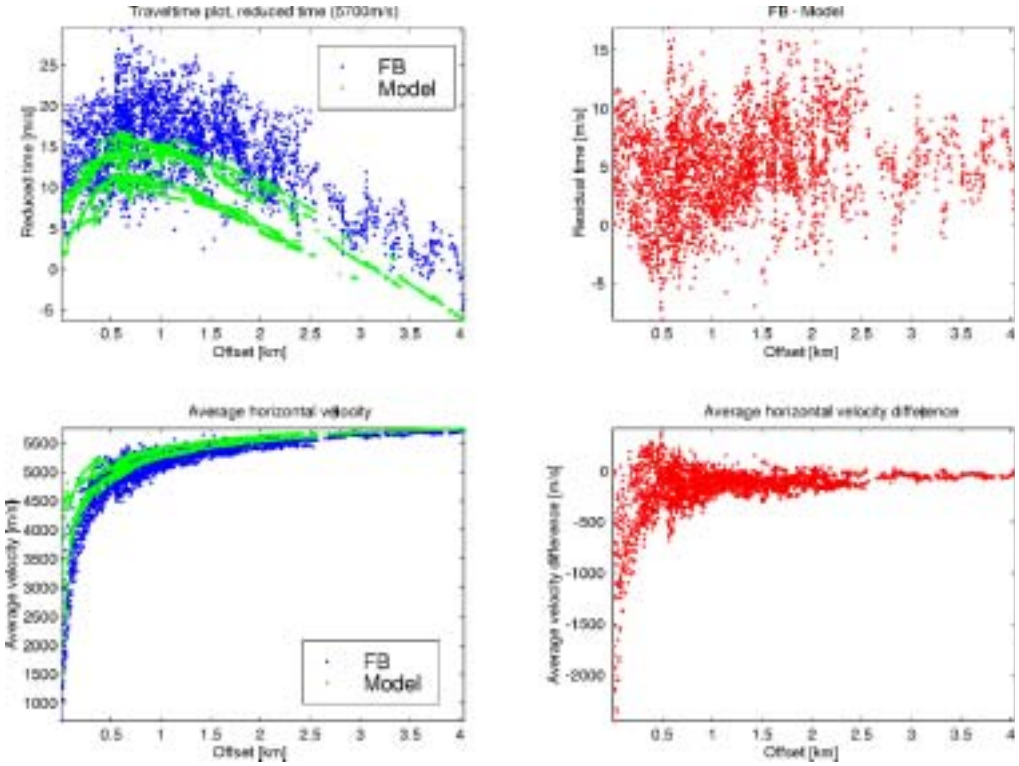


*Figure 4-20. Comparison of observed first arrivals (FB) with those calculated (Model) for the initial model.*

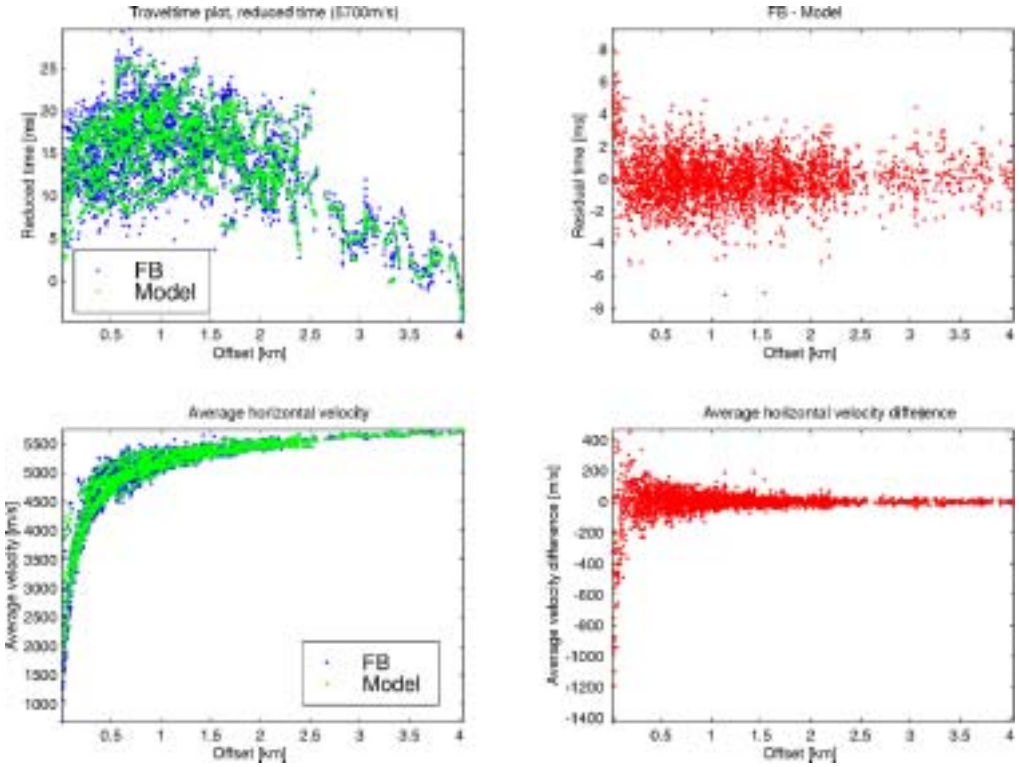


*Figure 4-21. Comparison of observed first arrivals (FB) with those calculated (Model) for the final model after 10 iterations shown in Figures 4-22 and 4-23.*

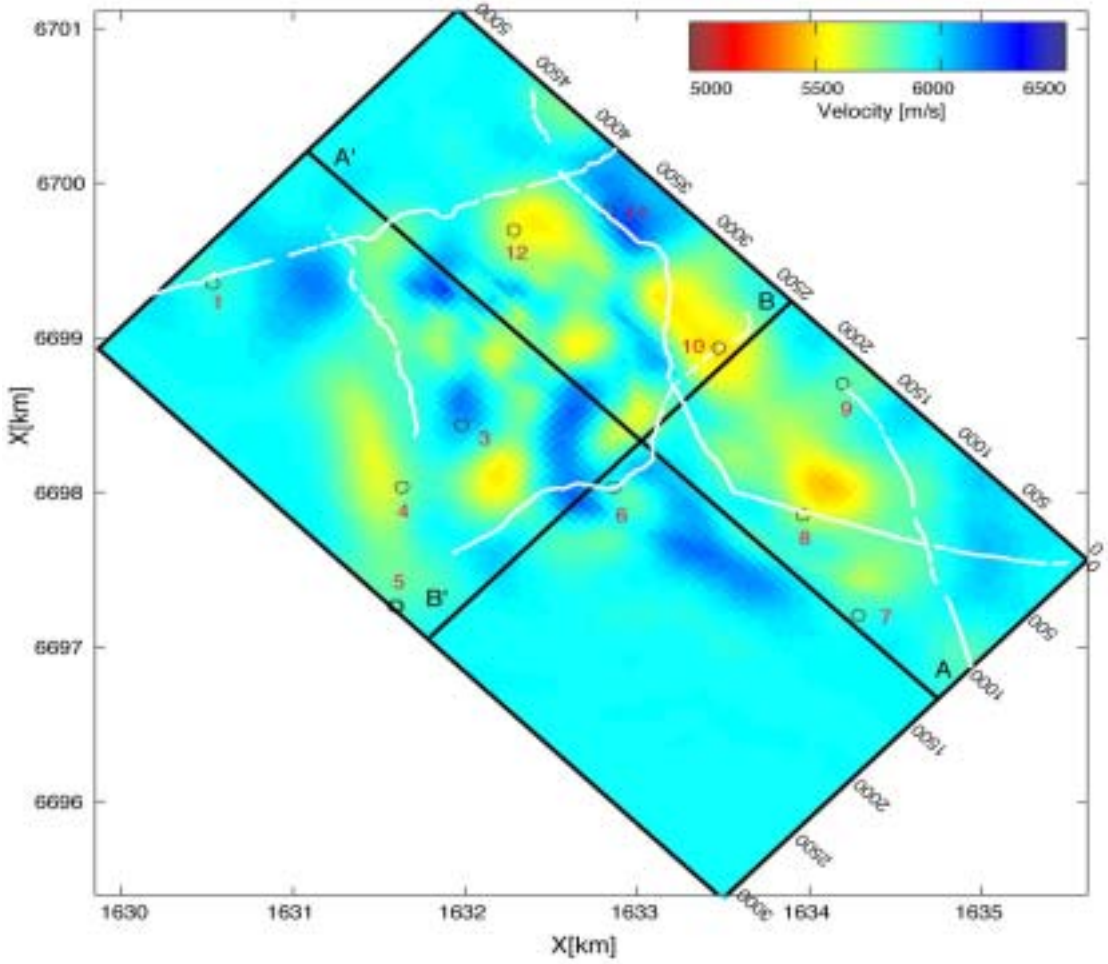


*Figure 4-22. Plan view of the 3D P-wave velocity field at a depth of 175 m. Shots used in the inversion are shown as white dots.*

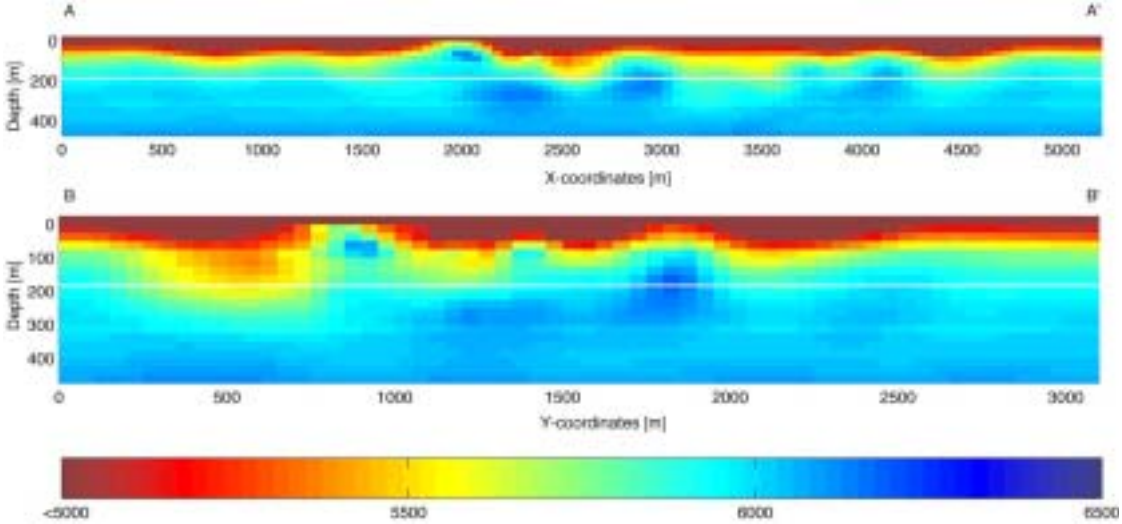


*Figure 4-23. Vertical sections of the 3D P-wave velocity field along profiles AA' and BB' in Figure 4-22.*

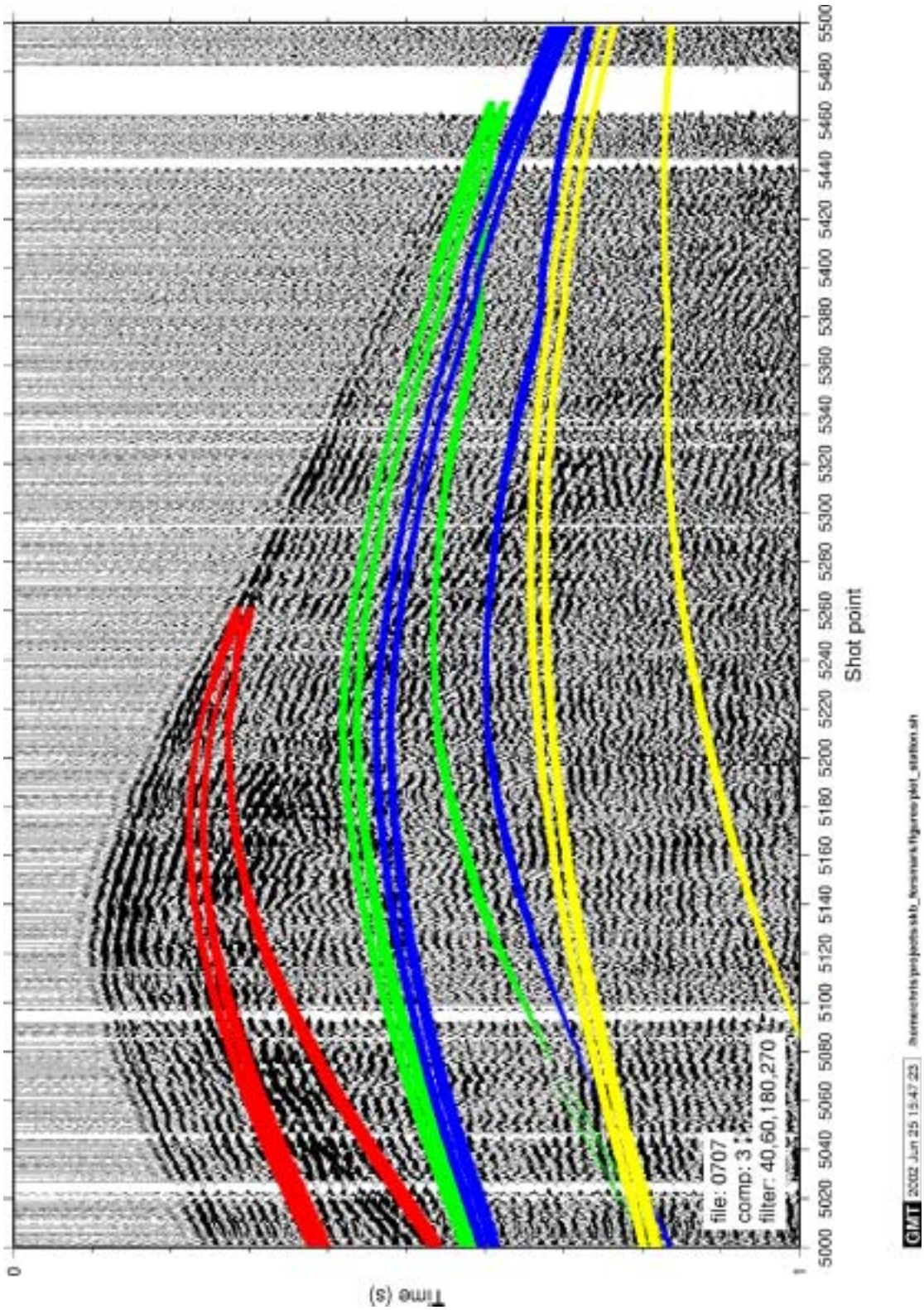


*Figure 4-24. Vertical component seismograms from profile 5 recorded at station 7 with synthetic seismograms from the set B reflectors overlain. B1-red, B2-green, B3-blue, B5-yellow. PP and PS reflections have been modeled.*

## 4.3. Predictions for deep borehole KFM01

Intersection points of the picked reflectors with the projection of borehole KFM01 downwards are given in Table 4-2. Note that the upper 0.35 s (c. 1000 m) is only weakly reflective where profiles 1 and 4 cross, indicating that no strong discontinuities may be expected to be drilled in the upper 1000 m at this location. The clearest reflection near the borehole in the upper 350 ms is found at about 0.1 s between CDPs 100 and 200 on profile 4 (Figure 3-10). This reflection may be correlated to the A2 reflector or to the B4 reflector from profiles 3 and 5. The B3 reflector also projects to the surface near borehole KFM01. Since no crossing profile exists across this reflector its true strike and dip near KFM01 cannot be determined directly from the stacked sections. The set G reflections are quite weak and their existence somewhat uncertain. Correlation with borehole logs and future borehole seismic studies will show whether they are of any importance. The set H reflectors consist of several reflectors with the approximate orientation given for the H1 and H2 reflectors in Table 4-2. Since they are not distinct event and their dip is high, the intersection points with borehole KFM01 are very approximate.

**Table 4-2. Predicted intersection points of KFM01 with those reflectors that project into the borehole shallower than 1500 m. Rank indicates how sure the observation of each reflection is on profiles that the reflection is observed on; 1 – definite, 2- probable, 3-possible.**

| *Reflector* | *Intersection depth* | *Strike* | *Dip* | *Rank* |
|---|---|---|---|---|
| Possible A2 | 0 | 80 | 22 | 2 |
| Possible B4 | 10 | 50 | 28 | 2 |
| G1 | 190 | 180 | 3 | 3 |
| G2 | 290 | 180 | 3 | 3 |
| G3 | 1070 | 0 | 2 | 3 |
| G4 | 1170 | 0 | 2 | 3 |
| H1 | 770 | 123 | 70 | 2 |
| H2 | 1050 | 123 | 70 | 2 |

## 4.4. Predictions for deep borehole KFM02

Intersection points of the picked reflectors with the projection of borehole KFM02 downwards are given in Table 4-3. The most prominent reflectors expected to be encountered in borehole KFM02 are the A2, F1 and B4 reflectors at about 470 m, 510 m and 980 m depth, respectively. The A3 reflector (expected penetration depth: 180 m) is not very clear on the seismic sections in the vicinity of the borehole where profiles 2 and 5 cross (Figure 4-11). The B2 and B3 reflectors are not very clear here either, but would be penetrated at about 600 m and 800 m depth, respectively, if they are present. If the steeply dipping H1 reflector can be extrapolated from profiles 1 and 4 then it is expected to be encountered at about 50 m in KFM02.

**Table 4-3. Predicted intersection points of KFM02 with those reflectors that project into the borehole shallower than 1500 m. Rank indicates how sure the observation of each reflection is on profiles that the reflection is observed on; 1 – definite, 2- probable, 3-possible.**

| *Reflector* | *Intersection depth* | *Strike* | *Dip* | *Rank* |
|---|---|---|---|---|
| A2 | 470 | 80 | 22 | 1 |
| A3 | 180 | 65 | 25 | 1 |
| B2 | 600 | 30 | 25 | 2 |
| B3 | 800 | 30 | 21 | 2 |
| B4 | 980 | 50 | 28 | 1 |
| B5 | 1390 | 50 | 25 | 2 |
| F1 | 500 | 20 | 20 | 2 |
| H1 | 50 | 123 | 70 | 3 |

## 4.5. Predictions for deep borehole KFM03

Intersection points of the picked reflectors with the projection of borehole KFM03 downwards are given in Table 4-4. Of the three planned boreholes, the reflections are the clearest in the vicinity of KFM03, therefore, predictions at depth are expected to be most accurate here. The A5 reflector is expected to be drilled at about 60 m. Between the A5 reflector and the A4 reflector the bedrock is fairly transparent, indicating no strong contrasts in elastic properties are present in the bedrock between 60 m and 370. Note that reflectors with dips greater than 60-70º may be present in this interval, but are not imaged on the seismic. Below 370 m the reflectivity increases significantly and numerous reflectors are expected to be drilled. The most prominent one is the B1 reflector at about 640 m. The A2 and A3 reflectors are less clear where profiles 3 and 5 cross, but should be drilled between 800 and 900 m. The very strong B2 reflector at 1370 m is deeper than the planned borehole depth.

**Table 4-4. Predicted intersection points of KFM03 with those reflectors that project into the borehole shallower than 1500 m. Rank indicates how sure the observation of each reflection is on profiles that the reflection is observed on; 1 – definite, 2- probable, 3-possible.**

| *Reflector* | *Intersection depth* | *Strike* | *Dip* | *Rank* |
|---|---|---|---|---|
| A2 | 900 | 80 | 22 | 1 |
| A3 | 800 | 65 | 25 | 1 |
| A4 | 370 | 65 | 25 | 1 |
| A5 | 60 | 75 | 30 | 1 |
| B1 | 650 | 30 | 25 | 1 |
| B2 | 1370 | 30 | 25 | 1 |
| B3 | 1430 | 30 | 21 | 1 |

# 5. Discussion and conclusions

## 5.1. Acquisition

Seismic data acquisition was carried out within the planned time frame and the study was finished a few days earlier than expected. Acquisition of the 3-component seismic data at the Orion stations required more man hours than expected and there were a number of problems in getting all of the Orion stations to function properly. If the Orion stations are to be used in the future then more attention needs to be paid to station selection and technical preparation. Station locations should be tested before final decision on where to place the stations. A study should also be made on using the SIL acquisition system (Bödvarsson et al., 1999) in conjunction with the Orion stations. This solution would imply that data from the Orion stations are temporarily integrated into the permanent Swedish Seismic Network.

## 5.2. Processing

Processing was carried out based on experience from previous SKB studies using high-resolution reflection seismics (Juhlin, 1995; Juhlin and Palm, 1999; Bergman et al, 2002). Similar parameters were used on the current data set as on these previous data sets. Electrical noise from the Forsmark power station required special care to be taken in choice of temporal filtering parameters, especially on profile 4.

Since all profiles contain reflections originating from out-of-the plane of the profiles migration has not been applied to the data. Migration is normally carried out to convert the time section to a depth section which is easier for the geologist to interpret. However, migrating the present data would give a false image of where the reflectors are located in space. Only 3D acquisition and processing would allow a true depth imaged to be obtained directly from the seismic data.

## 5.3. Interpretation

Since it is not possible to directly migrate the reflections to their true spatial position in the present data set a strategy based on seismic modeling has been used to locate the reflectors in the sub-surface. Focus has been on the most prominent reflections and weaker reflections close to where the first three deep boreholes are to be drilled. In the modeling carried out so far it has been assumed that the reflectors can be modeled as planes. This is only locally true. Therefore, extrapolation of reflectors to the surface is uncertain away from the profiles. The best extrapolations to the surface are for the set A reflectors along profiles 3 and 5 in the southeastern part of the survey area.

Towards the northwest the bedrock appears to be less reflective. This could be interpreted as a result of interference from the power station. However, the clear and strong reflections from about 1 second (3 km depth) suggest that signal penetration is generally not a severe problem. This implies that no major seismic discontinuities should be expected in borehole KFM01, however, weaker reflectors will be drilled in the upper 1000 m. In contrast, boreholes KFM02 and KFM03 should penetrate major reflectors. These reflectors probably represent either fracture zones or sheets of mafic rock. More detailed studies are required to discriminate between these two possibilities.

## 5.4. Future work

The combined reflection and refraction seismic data set obtained is generally of high quality and will be a useful research data set for the future. Even though this data set has not been exhaustively analyzed, additional seismic reflection studies in the area can be suggested. These are (Figure 5-1):

- Extension of profiles 4 and 5 to the north to map the A1 reflector and to cross and investigate the Singö zone with a crossing profile to correlate them (profile 6)
- Extension of profile 2 to the south to cross the major NW-SE striking topographic and magnetic anomalies
- A new NW-SE running (profile 7) to (i) map the reflection that projects up to the surface near KFM01 (possibly A2 or B4), (ii) investigate the bedrock SW of the Forsmark power plant and (iii) cross the projection of the A1 structure to the west
- Acquire borehole seismic data (VSP) in the deep boreholes to verify the surface seismic images and map steeply dipping reflectors

Research themes for the current data set which are highly relevant for SKB are:

- Study the effect of source coupling on the stacked sections
- Study the influence of the crooked line geometry on the stacked sections
- Correlate reflections on the Orion stations with stacked sections to allow limited 3D mapping
- Improvement of the 3D velocity model by including first arrival traveltimes from the reflection component of the study and possibly including first arrival S wave traveltimes

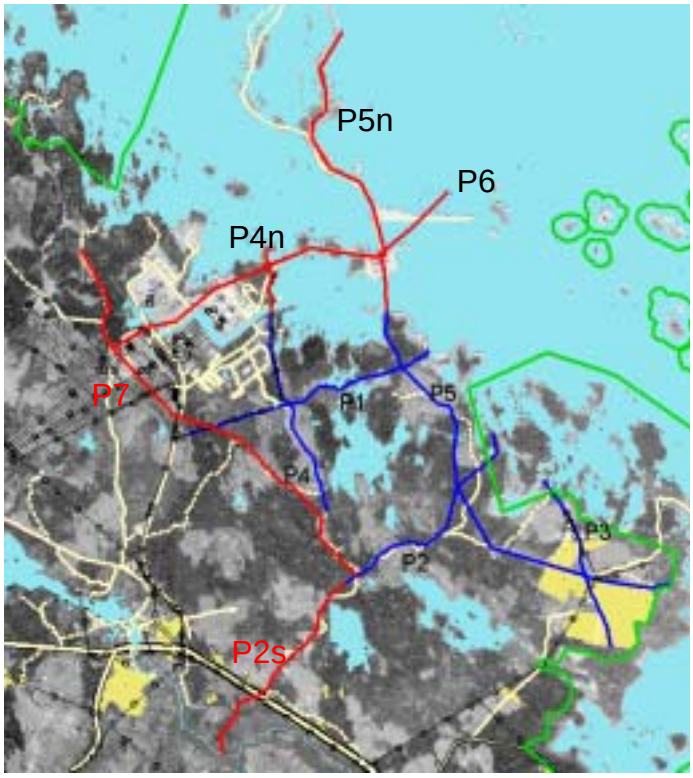


*Figure 5-1. Suggested additional (red lines) seismic profiles in the Forsmark area. Existing profiles /blue lines) are also shown.*

## References

Ayarza P., Juhlin C., Brown D., Beckholmen M., Kimbell G., Pechning, R., Pevzner, L., Pevzner, R., Ayala C., Bliznetsov, M., Glushkov A. and Rybalka A., 2000. Integrated geological and geophysical studies in the SG4 borehole area, Tagil Volcanic Arc, Middle Urals: Location of seismic reflectors and source of the reflectivity, J. Geophys. Res.: 105, 21333-21352.

Benz, H. M., Chouet, B. A., Dawson, P. B., Lahr, J. C., Page, R. A. and Hole, J. A., 1996. Three-dimensional P and S wave velocity structure of Redoubt Volcano, Alaska. J. Geophys. Res.: 101, 8111-8128.

Bergman, B., Juhlin, C.and Palm, H., 2002. Reflection seismic imaging of the upper 4 km of crust using small charges (15-75 grams) at Laxemar, southeastern Sweden. in press, Tectonophysics.

Bödvarsson, R., Rognvaldsson, S.T., Slunga, R., Kjartansson, E., 1999. The SIL data acquisition system - at present and beyond year 2000, Physics of the Earth and Planetary Interiors, 113: 89-101.

Juhlin, C., 1995. Imaging of fracture zones in the Finnsjön area, central Sweden, using the seismic reflection method. Geophysics: 60, 66-75.

Juhlin, C. and Palm, H., 1999. 3D structure below Ävrö island from high resolution reflection seismic studies, southeastern Sweden. Geophysics: 64, 662-667.

Tirén, S. A., Askling, P. and Wänstedt, 1999. Geologic site characterization for deep nuclear waste disposal based on 3D visualization. Engineering Geology: 52, 319-346.

Tryggvason,A., Rognvaldsson, S.T. And Flovenz, O. G., 2002. Three-dimensional imaging of the P and S wave velocity structure and earthquake locations beneath southwest Iceland., in press, Geophysical J. Int.

Wu, J., Milkereit, B. and Boerner, D., 1995. Seismic imaging of the enigmatic Sudbury structure. J. Geophys. Res.: 100, 4117-4130.